

UNIVERSITÀ
DI PAVIA

Dipartimento di Biologia e Biotecnologie "L. Spallanzani"

Laurea Magistralis in Neurobiology

The Role of α2 nAChR Subunit in Postsynaptic State-Dependent Plasticity within the Drosophila Mushroom Bodies

Supervisor:
Prof. Gerardo Biella

Co-supervisor:
Dr. Carlotta Pribbenow

Experimental thesis by
Marco Turrin

Academic Year 2025/2026

Thesis title

ENG The Role of α2 nAChR Subunit in Postsynaptic State-Dependent Plasticity within the Drosophila Mushroom Bodies

ITA Il Ruolo della Subunità nAChR α2 nella Plasticità Postsinaptica Stato-Dipendente nei Corpi Fungiformi di Drosophila

To my family and to my lifelong friends,
always with me no matter the distance.
And to the wonderful people I met along the way in Berlin,
who made this journey so much more than a thesis, turning it into the start of a new life.

Abstract

Synaptic strength in the brain is not only adjusted during learning: postsynaptic mechanisms also allow synapses to be tuned by an animal's broader internal, physiological state. At Drosophila mushroom body output synapses, the nicotinic acetylcholine receptor subunit α2 is an established mediator of this kind of postsynaptic, activity-dependent plasticity in the context of associative memory. Whether the same subunit also supports state-dependent plasticity more generally — adjusting synaptic strength in response to a purely physiological, non-associative pressure, rather than a trained association — is the broader question this thesis addresses. Sleep pressure and feeding state were chosen as the physiological variables to test this question, since they impose a homeostatic demand on this circuit without explicit training, and since sleep deprivation is known to increase MBON-γ2α′1's electrical activity (Sitaraman et al., 2015) while reducing its presynaptic KC contact number (Weiss and Donlea, 2021) — a pattern a purely presynaptic account cannot easily explain. Using an endogenously EGFP-tagged α2 reporter line, α2 expression was quantified across all ten mushroom body output compartments in a 2×2 factorial design crossing sleep deprivation with food deprivation (CNTRL, SD, FD, FDSD; n = 14–20 flies per group). Sleep deprivation significantly increased α2-EGFP fluorescence at four compartments — γ5, γ2, γ1, and β1 — a compartment-specific pattern inconsistent with a nonspecific, brain-wide effect. Food deprivation alone produced no change anywhere, but unexpectedly abolished the sleep-deprivation effect at all four compartments when combined with it, indicating that feeding state gates, rather than simply adds to, this postsynaptic response. At MBONγ5β′2a/M6, where activity was previously shown to decrease after sleep deprivation, the α2 increase is difficult to reconcile with a simple postsynaptic account. A computational model combining this thesis's α2 data with published presynaptic and electrophysiological data under one shared coupling constant shows this reconciliation is quantitatively impossible without an additional inhibitory input, plausibly from MVP2 — a specific, falsifiable prediction for future work. Together, these results show that α2-dependent postsynaptic plasticity is not specific to associative learning but is also recruited by purely homeostatic states, uncover an undocumented interaction between sleep pressure and feeding state, and turn a long-standing puzzle in this circuit into a concrete, testable hypothesis.

Abstract (Italiano)

La forza sinaptica nel cervello non viene regolata solo durante l'apprendimento: meccanismi postsinaptici permettono alle sinapsi di essere modulate anche dallo stato fisiologico interno dell'animale, più in generale. Nelle sinapsi di output del corpo fungiforme di Drosophila, la subunità del recettore nicotinico dell'acetilcolina α2 è un mediatore consolidato di questo tipo di plasticità postsinaptica, attività-dipendente, nel contesto della memoria associativa. Se la stessa subunità sostenga anche una plasticità stato-dipendente in senso più generale — regolando la forza sinaptica in risposta a una pressione puramente fisiologica, non associativa, piuttosto che a un'associazione appresa — è la domanda più ampia a cui questa tesi cerca di rispondere. La pressione indotta dalla deprivazione di sonno e lo stato nutrizionale sono state scelte come variabili fisiologiche per testare questa domanda, poiché impongono una richiesta omeostatica su questo circuito senza alcun addestramento esplicito, e poiché è noto che la deprivazione di sonno aumenta l'attività elettrica di MBON-γ2α′1 (Sitaraman et al., 2015) riducendo al contempo il suo numero di contatti presinaptici con i Kenyon cells (Weiss e Donlea, 2021) — un pattern che un resoconto puramente presinaptico non riesce a spiegare facilmente. Utilizzando una linea reporter con tag endogeno EGFP per α2, l'espressione di α2 è stata quantificata in tutti e dieci i compartimenti di output del corpo fungiforme, in un disegno fattoriale 2×2 che incrocia deprivazione di sonno e deprivazione di cibo (CNTRL, SD, FD, FDSD; n = 14–20 moscerini per gruppo). La deprivazione di sonno ha aumentato significativamente la fluorescenza di α2-EGFP in quattro compartimenti — γ5, γ2, γ1 e β1 — un pattern compartimento-specifico incompatibile con un effetto aspecifico esteso a tutto il cervello. La sola deprivazione di cibo non ha prodotto alcun cambiamento in nessun compartimento, ma, inaspettatamente, ha abolito l'effetto della deprivazione di sonno in tutti e quattro i compartimenti quando le due venivano combinate, indicando che lo stato nutrizionale regola, piuttosto che limitarsi ad aggiungersi, questa risposta postsinaptica. In MBON-γ5β′2a/M6, dove l'attività era stata precedentemente mostrata diminuire dopo la deprivazione di sonno, l'aumento di α2 è difficile da conciliare con un semplice resoconto postsinaptico. Un modello computazionale che combina i dati di α2 di questa tesi con dati presinaptici ed elettrofisiologici pubblicati, sotto un'unica costante di accoppiamento condivisa, mostra che questa

riconciliazione è quantitativamente impossibile senza un ulteriore input inibitorio, plausibilmente proveniente da MVP2 — una predizione specifica e falsificabile per lavori futuri. Nel loro insieme, questi risultati mostrano che la plasticità postsinaptica α2-dipendente non è specifica dell'apprendimento associativo ma viene reclutata anche da stati puramente omeostatici, rivelano un'interazione non ancora documentata tra pressione di sonno e stato nutrizionale, e trasformano un enigma di lunga data in questo circuito in un'ipotesi concreta e verificabile.

Table of Contents

1. Introduction **1**

1.1 Synaptic plasticity: the molecular substrate for learning and behavioural adaptation 1

1.2 Drosophila as a model organism; mushroom body anatomy and physiology 4

1.3 Postsynaptic plasticity at MBON synapses; role of nAChRs 9

1.4 Endogenous states as modulators of mushroom body plasticity: hunger, sleep, and metaplasticity 16

1.5 The mushroom body sleep homeostasis: segregated microcircuits and an open question about the postsynaptic side 19

2. Aim of the Work **25**

3. Methods **28**

3.1 Fly stocks and husbandry 28

3.2 Sleep deprivation / food deprivation paradigm 28

3.3 Tissue processing, confocal imaging, and ROI quantification 31

3.4 Statistical analysis pipeline 33

4. Results **35**

4.1 Sleep deprivation increases postsynaptic α2 expression in a subset of mushroom body compartments 35

5. Discussion **37**

5.1 A local feedback hypothesis linking presynaptic contact loss to postsynaptic α2 upregulation 37

5.2 Hunger state gates the postsynaptic response to sleep deprivation 42

5.3 A quantitative gain-modulation model, and the MVP2 inhibitory-tone hypothesis 48

5.3.1 Data sources and a first, important limitation 48

5.3.2 Model structure 49
5.3.3 Fitting the model: where a purely local account fails, and what fixes it 50
5.3.4 A speculative, same-dataset rationale for the MVP2 hypothesis 53
5.3.5 An open experimental question 54
5.3.6 Assumptions and limitations of the model 55
6. Conclusions **57**
6.1 Limitations 57
6.2 Future directions 61
References **67**

1. Introduction

1.1 Synaptic plasticity: the molecular substrate for learning and behavioural adaptation

Every output a nervous system produces — a motor action, a perceptual judgment, a memory, an emotional state — is ultimately the product of computation performed by circuits of neurons connected through synapses. This is not a metaphor of convenience but a claim about mechanism: the architecture of a neural circuit, defined by which neurons connect to which, with what sign, and with what strength, determines what that circuit can compute, and it is this computation, running on the physical substrate of the circuit, that constitutes the nervous system's function (Bargmann and Marder, 2013). Cognition, behavior, and experience are not added on top of circuit activity; they are what a particular pattern of circuit activity, shaped by a particular connectivity architecture, is.

This identity, rather than a merely causal relationship, is worth stating explicitly, because the argument that follows depends on it. It is not that a given circuit architecture causes a percept, a memory, or a behavioral choice to arise as some further, separate phenomenon; the percept, the memory, and the choice are the activity of that circuit, unfolding under a given input according to the connections and weights that define it. Two circuits with identical connectivity and identical synaptic weights would, by construction, produce identical output under identical input — there is no additional ingredient left over to account for. Conversely, any two circuits that produce different output under the same input must differ in their connectivity, their synaptic weights, or both. On this view, the entire behavioral and cognitive repertoire available to an organism at a given moment is fully specified by the current state of its circuits, and the question of what shapes cognition, perception, and behavior becomes, without residue, the question of what shapes circuit architecture.

Circuit architecture is shaped across two mechanistically continuous timescales. During development, an initial draft of circuit connectivity is laid down under substantial genetic control, but its refinement — the elimination of exuberant connections, the strengthening of some synapses and the weakening or loss of others — is itself activity-dependent, and proceeds through the same class of

synaptic mechanisms that operate later in life (Katz and Shatz, 1996). This developmental sculpting is often concentrated within bounded critical periods, windows during which circuits are especially sensitive to experience before consolidating into a comparatively more stable configuration (Hensch, 2005). Once this initial architecture is in place, synaptic plasticity does not switch off: throughout adult life, the same class of activity-dependent change in synaptic weight continues to modify circuit architecture in response to ongoing experience — at a smaller scale, and typically without the wholesale rewiring seen earlier in development, but through the same underlying molecular logic. Developmental and adult plasticity are, in this sense, the same mechanism acting on the same substrate at different moments of an organism's life: development builds the computational architecture, and, for as long as the organism lives, synaptic plasticity remains essentially the only means by which that architecture — and with it, the totality of the organism's behavior, cognition, and perception — can be reshaped.

Taken to its natural conclusion, this argument implies that synaptic plasticity is not merely a mechanism for encoding discrete pieces of information, but the natural phenomenon underlying identity and selfhood. Character, personality, and what is most commonly described as one's sense of self are not qualities superimposed on a nervous system from without; they are properties of the particular configuration that system's synaptic connections have come to take over a lifetime of experience. There is no self to be found independently of that configuration, and no such configuration that does not, in some sense, constitute a self (LeDoux, 2002). Whatever an organism is, in the psychological sense of that term, is inseparable from the plastic history of its circuits.

Genetic programs can specify the coarse wiring of a circuit, but they cannot specify, in advance, the particular sequence of experiences an individual will have; the architecture must therefore remain modifiable after it is built if it is to come to reflect that individual history at all. This is not merely a conceptual necessity but a quantitative one. The human genome comprises roughly 3 × 109 base pairs and can therefore specify, at an information-theoretic maximum, on the order of 109 bits — a few hundred megabytes. The adult human brain, by contrast, contains on the order of 1011 neurons, each forming on the order of 103 synaptic connections; specifying the strength and identity of each of these connections independently would require

several orders of magnitude more information than the genome can carry (Changeux and Danchin, 1976; Zador, 2019). The genome, in other words, cannot by itself specify a fully wired brain: it can set out general rules and constraints, but the remaining information needed to instantiate a functioning circuit must be supplied from outside the genome altogether. Experience-driven synaptic plasticity is the principal route by which this additional information enters the system — humans acquire and retain new information at an estimated rate of only about two bits per second, yet sustained over a lifetime this amounts to on the order of 109 bits of learned information (Landauer, 1986), a quantity on the same order as the genome itself, and a further illustration of how much of what a nervous system ultimately becomes must be written into it through plasticity rather than specified in advance.

It is synaptic plasticity that provides the molecular mechanism by which this modification occurs (Hebb, 1949; Bliss and Lømo, 1973). In this view, synaptic plasticity is not one mechanism among several by which experience influences the brain; it is essentially the mechanism by which a computational architecture that is initially specified by genes becomes, over time, an architecture that also encodes the organism's individual history — what Kandel (2001) described as a continuous dialogue between genes and synapses.

Therefore, if behavioral and cognitive output is nothing other than what a given circuit architecture computes, and synaptic plasticity is essentially the sole mechanism by which that architecture is reshaped by experience, then understanding any instance of experience or state-dependent change in behavior requires identifying the underlying change in synaptic weights, and, where possible, its molecular implementation.

1.2 Drosophila as a model organism; mushroom body anatomy and physiology

Much of the experimental logic of this research field depends on advantages that are specific to *Drosophila melanogaster* as a model organism. Over a century of genetic work on the fly has produced an unusually complete toolkit for manipulating identified neurons. The GAL4/UAS binary expression system allows a transgene of choice to be expressed within a genetically defined population of cells (Brand and Perrimon, 1993), and its intersectional refinement, the split-GAL4 method, reconstitutes a functional transcription factor only in cells that satisfy two independent expression patterns simultaneously (Pfeiffer et al., 2010) — making it possible, in practice, to restrict a manipulation to a single neuron type per brain hemisphere. This level of genetic access to identified cells, routine in *Drosophila*, remains difficult to achieve in most vertebrate systems. The fly's relevance is not confined to insect biology: nearly 75% of genes associated with human disease have a recognizable *Drosophila* ortholog (Reiter et al., 2001), and the fly has repeatedly served, across a century of use, as an experimental system whose findings generalize to vertebrate, including human, neuroscience (Bellen, Tong, and Tsuda, 2010).

These genetic advantages are compounded by practical ones, which have been particularly important to carry out this work in such a limited timeframe: a short generation time, low cost of maintenance, and the ability to generate and phenotype large numbers of animals, which together support the kind of highly powered, systematically controlled behavioral experiments that this thesis's design also relies on. Just as importantly, the *Drosophila* central brain, on the order of 10^5 neurons, is small enough that entire circuits — not just individual cell types, but the complete set of cell types that make up a circuit, their connectivity, and their function — can be described exhaustively. It is this combination of genetic precision and circuit-level tractability that makes it possible to study a specific molecular event, such as a change in postsynaptic receptor expression, in the context of the full circuit it belongs to, rather than in isolation.

The mushroom body: input and anatomical organization

The mushroom body (MB), is the principal site of associative learning and memory in the insect brain. Olfactory information reaches the MB by way of roughly 50 antennal lobe glomeruli, whose projection neurons synapse, in a non-stereotyped pattern that differs from individual to individual, onto the dendrites of the Kenyon cells (KCs) in the MB calyx (Aso et al., 2014). Each fly has on the order of 2000 KCs per hemisphere — close to 10% of all neurons in the central brain — and any given odor activates only a sparse, largely non-overlapping subset of them, so that odor identity is represented combinatorially across the KC population rather than by any single, dedicated cell (Aso et al., 2014).

The parallel axonal fibers of the KCs run through the peduncle and split into anatomically distinct lobes — the vertical α/α′ lobes and the horizontal β/β′/γ lobes — which are further subdivided into 15 compartments along their length, plus one additional compartment in the core of the distal peduncle (pedc), for 16 compartments in total (Aso et al., 2014). This compartmentalization is not incidental: each compartment is defined by the convergence, onto the same stretch of KC axon, of the dendrites of one or more mushroom body output neurons (MBONs) and the axon terminals of one or more dopaminergic neurons (DANs), so that the MB lobes function less as a single uniform structure and more as a parallel array of largely independent computational units.

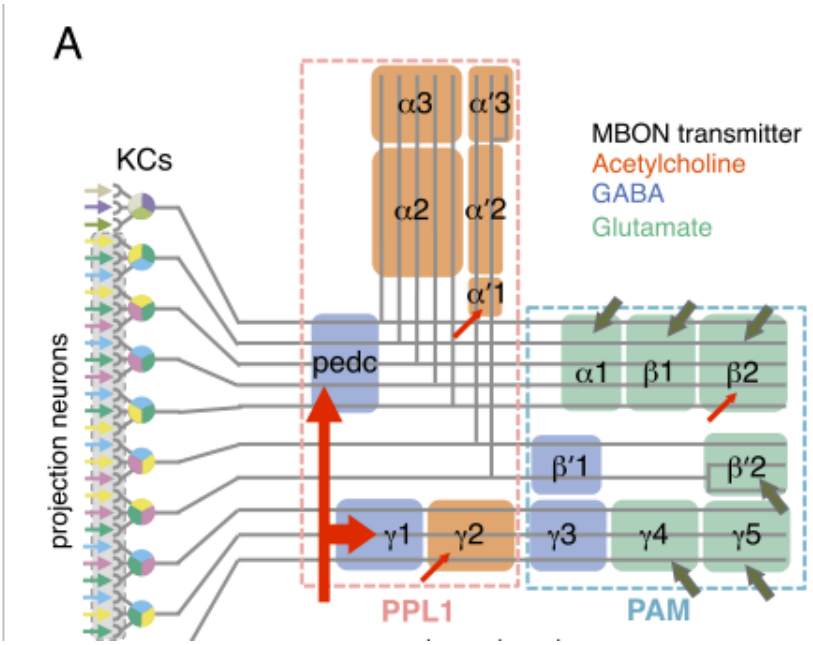


Fig. 1.1 The mushroom body compartment map. Kenyon cell axons (gray) run through the pedc compartment and branch into the α/α' and β/β'/γ lobes, subdivided into 16 compartments. Compartments are color-coded by the neurotransmitter of the MBON(s) that arborize there (orange, acetylcholine; blue, GABA; green, glutamate). PPL1 dopaminergic neurons (red arrow) convey punishment signals to a subset of compartments; PAM dopaminergic neurons (gray arrows) convey reward signals to a largely non-overlapping subset. Adapted from Aso et al. (2014)

Output logic: MBONs, dopamine, and compartment-specific plasticity

The output of the entire MB is carried by a surprisingly small number of neurons: 34 MBONs of 21 cell types per hemisphere, each with dendrites restricted to one or a few compartments, collectively conveying information to a handful of downstream brain regions — the crepine, the superior medial and lateral protocerebrum, the superior intermediate protocerebrum, and the lateral horn (Aso et al., 2014). MBONs are not functionally interchangeable: cell types releasing glutamate tend to promote avoidance and wakefulness when activated, while cholinergic and GABAergic cell types tend to promote approach and sleep, and it is the balance of activity across this population — rather than the response of any individual MBON — that is thought to encode the learned valence of a stimulus and bias the fly's subsequent behavior (Aso et al., 2014).

This population code is written by dopamine. DANs innervating the MB lobes fall into two main clusters with largely opposing behavioral roles: PPL1 neurons, whose activation conveys punishment, and PAM neurons, whose activation conveys reward, each innervating a distinct and largely non-overlapping subset of compartments (Aso et al., 2014). When KC activity representing a given stimulus

coincides, within a compartment, with a dopaminergic signal, the strength of the corresponding KC-to-MBON synapse is altered — depressed in most documented cases — so that the MBONs postsynaptic to that compartment change their response to that stimulus in subsequent encounters. This coincidence-detection mechanism is, in effect, a dopamine-gated, compartment-restricted instance of the Hebbian plasticity introduced in Section 1.1: KC activity supplies the presynaptic term, dopaminergic input supplies the reinforcement term, and the resulting change in synaptic weight at that specific KC-MBON synapse is what allows the MBON ensemble, and therefore the circuit's behavioral output, to come to reflect the fly's individual history with that stimulus.

A further point deserves emphasis here: unlike the principal excitatory neurons of the most extensively studied vertebrate circuits, KCs are cholinergic: acetylcholine, not glutamate, is the transmitter released at KC-to-MBON synapses (Barnstedt et al., 2016), making nicotinic acetylcholine receptors (nAChRs) — rather than AMPA- or NMDA-type glutamate receptors — the principal postsynaptic receptor class through which MBONs read out KC input (Owald and Waddell, 2015). This is not a peripheral biochemical detail: because nAChRs occupy, within this circuit, functionally the same position that AMPA and NMDA receptors occupy at vertebrate excitatory synapses, any postsynaptic modification of MB output synapses is necessarily implemented through changes in the fly's nAChR complement — a parallel this thesis returns to directly in Section 1.3, where a specific pair of nAChR subunits, α2 and α5, is argued to play a role functionally analogous to that of AMPA and NMDA receptors, respectively, in synaptic plasticity at these synapses.

The nAChR gene family is far from a single entity: *Drosophila* expresses at least seven nicotinic α subunits (α1-α7), and a CRISPR-based collection of fly lines now exists in which each α subunit is individually tagged with GFP at its own endogenous genomic locus, allowing its expression to be visualized under the control of its native promoter rather than an exogenous driver (Pribbenow et al., 2022). The experiments I performed make use of the α2 member of that collection: an α2-EGFP line in which EGFP expression reports the fly's own endogenous, constitutive α2 expression throughout the brain, rather than being restricted to a pre-selected population of neurons by a GAL4 or LexA driver. This is, deliberately, a simple genetic tool — a

reporter of receptor abundance rather than a targeted manipulation — but that simplicity is precisely what makes it possible to quantify α2 signal within any MB compartment of interest, including compartments housing more than one MBON type, without first having to identify and drive a compartment-specific line for each one.

Critically, the MBON population's role is not restricted to associative memory. Using the same anatomical and genetic framework, Aso et al. (2014) showed that MBONs also bidirectionally regulate sleep: activating glutamatergic MBONs such as MBON-γ5β′2a promotes wakefulness, while activating cholinergic and GABAergic MBONs such as MBON-γ2α′1 promotes sleep, with both classes converging onto the same downstream regions (the superior medial protocerebrum and crepine). The same output architecture that the MB uses to convert a learned association into a behavioral bias is therefore also used to regulate an ongoing internal state — a finding developed further, and made the direct subject of Section 1.5, by Sitaraman et al. (2015).

A shared circuit logic across phyla

The MB's organization — sparse, high-dimensional expansion coding at the KC layer feeding into a much smaller population of compartmentalized, neuromodulator-gated output neurons — is not unique to insects. Structurally and computationally comparable motifs appear in the mammalian cerebellum (granule cells expanding input dimensionality before convergence onto Purkinje cells) and in the hippocampal dentate gyrus (sparse granule cell coding upstream of associative circuits), and the parallel is close enough that principles first worked out in the fly MB have informed models of these vertebrate circuits, and vice versa (Modi, Shuai, and Turner, 2020). This is not offered as a claim that the MB and the hippocampus are homologous structures, but as a reason to expect that mechanisms of compartment- and synapse-specific plasticity identified in the MB — including the postsynaptic mechanisms that are the focus of this thesis — may reflect solutions to computational problems that recur across nervous systems built on very different evolutionary starting points.

1.3 Postsynaptic plasticity at MBON synapses; role of nAChRs

Synaptic plasticity, broadly defined as activity-dependent or neuromodulator-dependent changes in the efficacy of synaptic transmission, is widely regarded as the cellular substrate of learning, memory, and, more generally, of the nervous system's capacity to adjust its function to experience (Glanzman, 2010; Korte and Schmitz, 2016; Nicoll, 2017). Such changes can, in principle, be implemented on either side of the synapse: presynaptically, through altered probability or amount of neurotransmitter release, or postsynaptically, through the rearrangement, trafficking, or exchange of neurotransmitter receptors and their associated scaffolding machinery. In the vertebrate central nervous system, both mechanisms are well established, and postsynaptic plasticity in particular has been characterized in considerable molecular detail: NMDA-receptor-dependent induction of long-term potentiation and depression is expressed, at least in part, through changes in the number, subunit composition, and synaptic anchoring of AMPA receptors, coordinated by postsynaptic scaffold proteins such as PSD-95 (Korte and Schmitz, 2016; Nicoll, 2017).

In invertebrates, by contrast, memory-relevant synaptic plasticity has traditionally been considered a predominantly presynaptic phenomenon. In Drosophila melanogaster, where associative memories are stored within the mushroom bodies (MBs) at the synapses between Kenyon cells (KCs) and MB output neurons (MBONs), decades of work have pointed to presynaptic mechanisms — modulated by dopaminergic input onto anatomically discrete MB compartments — as the principal site of memory-related synaptic weight change (Owald and Waddell, 2015; Cohn et al., 2015; Hige et al., 2015). Whether postsynaptic mechanisms contribute meaningfully to invertebrate synaptic plasticity, as they do in vertebrates, remained comparatively unclear. This is a non-trivial question: it asks whether postsynaptic plasticity is a conserved, general-purpose feature of nervous systems that happens to be implemented with a different receptor chemistry in different phyla (nicotinic acetylcholine receptors, nAChRs, in Drosophila, versus glutamate receptors in vertebrates), or whether it is instead a vertebratespecific elaboration.

As introduced in Section 1.2, this receptor-chemistry question is not incidental: acetylcholine, not glutamate, is the principal fast excitatory transmitter at

KC-to-MBON synapses (Barnstedt et al., 2016), which places nicotinic acetylcholine receptors (nAChRs), rather than AMPA- or NMDA-type glutamate receptors, in the position of principal postsynaptic receptor class at the MB output synapse (Owald and Waddell, 2015). Answering the question of whether postsynaptic plasticity operates at this synapse therefore first requires a basic description of what an insect nAChR actually is, at the level of protein structure and subunit composition, before turning to the specific subunit — α2 — this thesis is concerned with. Like their vertebrate counterparts, insect nAChRs belong to the Cys-loop superfamily of ligand-gated ion channels and assemble as pentamers: five subunits arranged around a central cation-permeable pore, each subunit contributing an N-terminal extracellular ligand-binding domain and four transmembrane passes (Rosenthal and Yuan, 2021). Only subunits bearing a pair of adjacent extracellular cysteine residues are classified as α subunits; these contribute the principal face of the ACh-binding pocket (Loops A-C), while non-α subunits contribute a complementary face (Loops D-F) that helps position the ligand without binding it directly (Rosenthal and Yuan, 2021). Drosophila carries ten nAChR genes in total — seven α subunits (Dα1-Dα7) and three non-α, β subunits (Dβ1-Dβ3) — roughly a third to a half of which show clear sequence similarity to their vertebrate homologs (Dupuis et al., 2012; Gundelfinger and Hess, 1992). Unlike the vertebrate neuromuscular junction, where nAChRs sit at a peripheral, cholinergic-to-muscle synapse, Drosophila nAChRs are confined to the CNS, where they serve as the primary means of fast excitatory neurotransmission between neurons (Gundelfinger and Hess, 1992) — functionally, it might be proposed to be the insect equivalent of the role AMPA and NMDA receptors play at central glutamatergic synapses in vertebrates.

This nine-fold (seven α plus, functionally, up to three β) subunit repertoire does not assemble indiscriminately. Sequence comparisons group the subunits into distinct phylogenetic clusters — for example, Dα5, Dα6, and Dα7 form an ‘α7-like’ cluster named for their vertebrate counterpart, and, unusually among the family, these subunits are able to form functional homomeric channels — composed of a single subunit type — in addition to heteromeric ones (Lansdell et al., 2012; Rosenthal and Yuan, 2021). Most other Drosophila nAChR subunits, by contrast, appear to require co-assembly with at least one other subunit type to form a functional channel. Of particular relevance here, Dα1, Dα2, and Dβ2 form a three-gene genomic cluster

that is conserved in mammals, which carry homologs of the same three subunits at a syntenic locus (Rosenthal and Yuan, 2021) — one of several lines of evidence, alongside coimmunoprecipitation of Dα1 with Dα2 from head membrane extracts, that these subunits can co-assemble in vivo. α2 itself is not narrowly restricted in its expression: early in situ hybridization work found Dα2 transcript broadly distributed across the brain and ventral nerve cord (Rosenthal and Yuan, 2021), consistent with a receptor subunit that is deployed widely across central cholinergic synapses rather than being restricted to a single circuit.

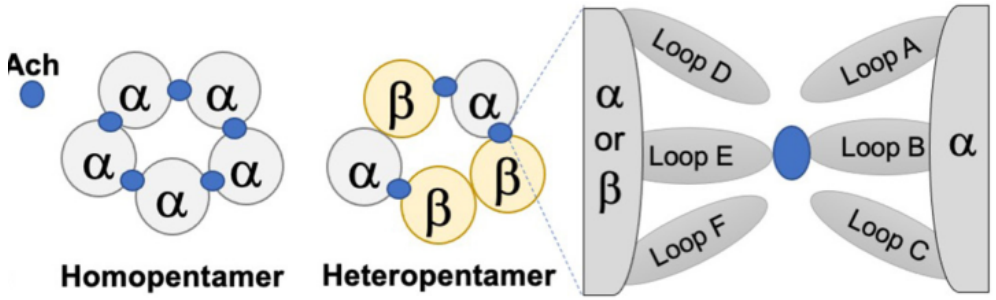


Fig. 1.2 Molecular architecture of Drosophila nAChRs: the two stoichiometric receptor classes — homopentamers (identical subunits) and heteropentamers (mixed α/β subunits) — and the principal (Loops A-C) / complementary (Loops D-F) face architecture of the ACh-binding interface. Adapted from Rosenthal and Yuan (2021), Figure 1D.

Within the MB specifically, Pribbenow et al. (2022) showed that α2, together with α5, α1, and the scaffold protein Discs large (Dlg), is expressed at the postsynaptic densities of MBONs, and that RNAi knockdown of these components in defined MBON types selectively impairs specific phases and types of associative memory. In the M4/M6 MBONs, which are required for appetitive learning, knockdown of α5 abolished both immediate short-term and middleterm appetitive memory, whereas knockdown of α2 left short-term memory intact but selectively abolished middle-term memory — a functional dissociation between the two subunits within the same neurons. In MVP2 MBONs, by contrast, α2 knockdown abolished immediate appetitive short-term memory, while α5 knockdown instead abolished immediate aversive short-term memory, indicating that the same pair of subunits can be recruited differently depending on both MBON identity and the valence and phase of the memory being formed (Pribbenow et al., 2022). This subunit-specific, MBON-specific pattern is itself evidence that the postsynaptic receptor complement of a KC-MBON synapse — not merely the identity of the presynaptic KC or the sign

of the dopaminergic reinforcement it receives — is part of what determines the memory-relevant properties of that synapse.

MBON	Subunit /protein	Memory type	Phase Tested	Effect of RNAi knockdown
M4/M6	α5	Appetitive	Immediate	Abolished
M4/M6	α5	Appetitive	3-hour (MTM)	Abolished
M4/M6	α2	Appetitive	Immediate	No effect
M4/M6	α2	Appetitive	3-hour (MTM)	Abolished
M4/M6	α1	Appetitive	3-hour (MTM)	Abolished
M4/M6	Dlg	Appetitive	3-hour (MTM)	Abolished
M4/M6	any tested	Aversive	Immediate	No effect (any subunit)
M4/M6	α7	Aversive	3-hour (MTM)	Abolished (other subunits: no effect)
MVP2	α2	Appetitive	Immediate (STM)	Abolished
MVP2	α5	Aversive	Immediate (STM)	Abolished
MVP2	Dlg	Aversive	Immediate (STM)	Abolished
α′3	α5	Familiarity(non-associative)	—	Familiarity memory abolished; α2 dynamics (FRAP) abolished
α′3	α2	Familiarity(non-associative)	—	Familiarity memory abolished

Table 1.1 Summary of nAChR subunit and Dlg RNAi knockdown effects on associative and non-associative memory across MBON types. MTM = middle-term memory; STM = short-term memory. Compiled from Pribbenow et al. (2022, eLife) and Pribbenow (2025, doctoral dissertation, Charité – Universitätsmedizin Berlin).

A hierarchical relationship between the two subunits reinforces this picture. Knocking down α5 (which, notably, is itself capable of forming homomeric channels; Lansdell et al., 2012) reduces the amount of α2 present at the synapse and abolishes the activity-dependent dynamics of α2 described below, whereas knocking down α2 has no reciprocal effect on α5 levels (Pribbenow et al., 2022) — placing α5 functionally upstream of α2 within the same postsynaptic density. α1 is a further, structurally relevant piece of this picture: in the M4/M6 MBONs, Pribbenow et al. (2022) found that later, middle-term phases of appetitive memory expression require both α1 and α2 (Table 1.1), raising the question of whether the two subunits act within the same receptor complex rather than independently. Precisely how α1 and α2 relate to one another structurally remains an open question, though heterologous expression work

has shown that Dα1 and Dα2 are capable of co-assembling with Dβ subunits into pharmacologically distinct heteromeric channels (Ihara et al., 2020), leaving open the possibility that the KC-MBON receptor complex found at a given compartment is a mixed, rather than a single-subunit, assembly.

Taken together, this body of work established that postsynaptic plasticity of cholinergic KCto-MBON synapses is both necessary and sufficient to support the induction and expression of appetitive and familiarity memories in Drosophila, and, critically, that this plasticity is not merely a passive downstream readout of presynaptic change (Pribbenow et al., 2022).

The strongest evidence for this last point — that postsynaptic plasticity can be conceptualized, and demonstrated, as a process in its own right, separable from presynaptic events — comes from an explant-brain preparation in which Pribbenow et al. (2022) bypassed the KCs entirely. With network activity suppressed by bath-applied tetrodotoxin, dopamine release was triggered optogenetically (CsChrimson-expressing dopaminergic neurons, red-light activation) while KC input to M6 dendrites was mimicked by focal, exogenous application of acetylcholine, and the resulting calcium response in M6 was read out directly. Postsynaptic calcium responses to a fixed acetylcholine pulse increased only when acetylcholine application had previously been paired with dopaminergic activation — not after acetylcholine alone or dopamine alone — and this induced potentiation was itself abolished by RNAi knockdown of α2 in M4/M6.

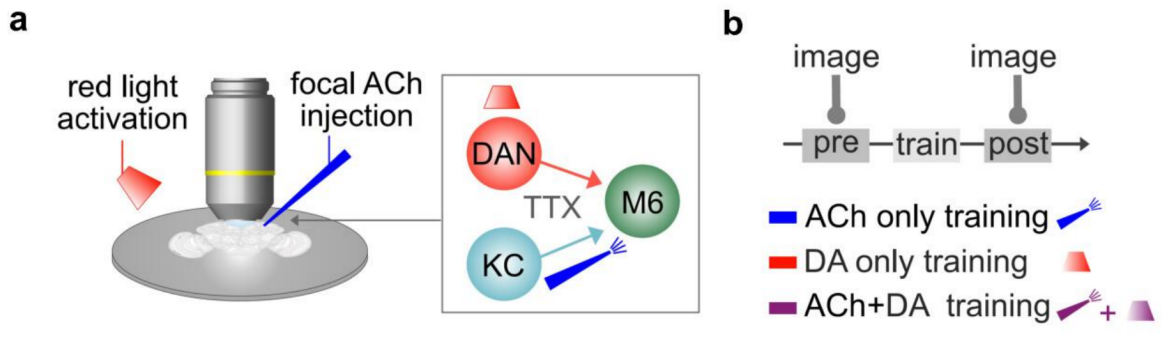


Fig. 1.3 The explant-brain preparation used to bypass the KC presynapse. (a) Optogenetic dopamine release (red light, CsChrimson-expressing DANs) is paired with focal, exogenous acetylcholine (ACh) injection directly onto M6 dendrites, with KCs and DANs otherwise silenced by bath-applied TTX. (b) Training/testing scheme: baseline (pre) and post-training ACh-evoked M6 calcium responses are compared across ACh-only, DA-only, and paired (ACh+DA) protocols. Adapted from Pribbenow et al. (2022), Figure 3a-b.

The logic of this design is what makes the ‘postsynaptic’ attribution possible. The acetylcholine pulse is not a presynaptic terminal capable of releasing more or less transmitter depending on activity history; it is a fixed, experimenter-controlled stimulus, delivered in the same amount before and after training. Because the input itself cannot change, any change in how M6 responds to that same fixed input must be a property of the receiving side — of M6's own receptor complement or excitability — rather than of anything upstream. Two further features of the preparation reinforce this attribution: TTX silences the entire network, so the real KCs cannot fire or release transmitter of their own accord, and the authors additionally show that the acetylcholine puff itself evokes no calcium transient in KC axons, meaning the stimulus does not even feed back onto the KCs it is standing in for. The pathway being tested for plasticity is specifically the efficacy of cholinergic transmission onto M6, with dopamine acting only as the paired reinforcement signal, not as the pathway under study. The authors themselves are careful to qualify what this experiment does and does not show. Because it relies on global, bath- or pipette-delivered acetylcholine rather than the sparse, single-synapse activation that would occur physiologically, they describe it explicitly as a proof-of-principle that does not necessarily reflect the receptor dynamics of an intact, behaving fly (Pribbenow et al., 2022). What the experiment demonstrates is that a postsynaptic mechanism, isolated from any presynaptic contribution, is sufficient to produce a lasting, dopamine-gated increase in M6's response to acetylcholine, and that this sufficiency depends on α2 — not that this isolated mechanism is the whole, or even the dominant, story at the intact KC-MBON synapse in vivo.

A complementary line of evidence came from in vivo fluorescence recovery after photobleaching (FRAP) of the endogenously tagged α2 subunit (α2GFP) in the β′2 and α′3 compartments: odor exposure alone significantly increased the rate at which bleached α2GFP fluorescence recovered — indicating increased receptor mobility into the synapse — while pairing the same odor with dopamine application suppressed this recovery, a signature consistent with dopamine-gated synaptic depression operating through altered α2 trafficking rather than through any change at the KC presynapse (Pribbenow et al., 2022).

The value of this finding lies not only in demonstrating that postsynaptic plasticity exists in an invertebrate cholinergic system, but in how closely its logic maps onto

the best-characterized postsynaptic plasticity mechanism in vertebrates. In the mammalian glutamatergic synapse, long-term potentiation is classically divided into an induction phase, gated by NMDA receptors acting as coincidence detectors, and a subsequent expression phase, in which the lasting change in synaptic strength is implemented through altered number, subunit composition, and synaptic anchoring of AMPA receptors (Nicoll, 2017). Pribbenow et al. (2022) proposed a directly analogous temporal receptor model for the Drosophila MB: the α5 subunit behaves as a functional counterpart to the NMDA receptor, occupying a gating position upstream in the pathway — its knockdown abolishes memory induction and, notably, also eliminates the activity-dependent dynamics of α2, without α5 itself showing comparable dynamics. The α2 subunit, by contrast, behaves as a functional counterpart to the AMPA receptor: it is the subunit whose in vivo dynamics actually track memory expression, it interacts with the postsynaptic scaffold Dlg in a manner reminiscent of the AMPAR–PSD-95 interaction that anchors AMPA receptors at vertebrate synapses, and its regulation is what is ultimately read out as a change in synaptic weight. In other words, α5 determines whether postsynaptic plasticity is triggered, while α2 determines what that plasticity looks like once expressed — the same division of labor that NMDA and AMPA receptors implement in vertebrates, despite the two systems sharing no receptor homology and using different neurotransmitters entirely.

This body of evidence positions α2 not as one candidate postsynaptic marker among several, but as the specific nAChR subunit whose in vivo dynamics constitute the readable signature of a lasting change in MB output synapse strength — a role it plays consistently across at least two distinct forms of learning, appetitive associative memory and non-associative familiarity learning, and one it plays downstream of, and dependent on, α5. The AMPA/NMDA parallel captures this division of labor conveniently, but the more direct point is empirical: α2 dynamics already generalize across different upstream drivers of plasticity within the MB, which is what makes this subunit, specifically, the natural entry point for examining postsynaptic plasticity at MB output synapses under conditions other than associative learning.

1.4 Endogenous states as modulators of mushroom body plasticity: hunger, sleep, and metaplasticity

The MB circuitry described so far has been treated, implicitly, as if it operated on a fixed set of rules: a given pattern of KC activity, paired with a given dopaminergic signal, produces a given change in a given KC-MBON synapse. In a real animal, however, this is not quite true. The same odor, the same reinforcement, and the same anatomical circuit can produce different behavioral outcomes, and by extension different synaptic outcomes, depending on the internal physiological state of the animal at the time — whether it is hungry or fed, rested or sleepdeprived. This is not merely a matter of the organism's behavior being biased on top of an otherwise unchanged computation; in several of the cases described below, the internal state changes which cells, which dopaminergic neurons, and by extension which induction and expression rules govern plasticity at that moment. This is the sense in which an internal state can act as a metaplastic variable: following Abraham and Bear's (1996) original formulation, metaplasticity refers to a change in the rules or thresholds that govern subsequent synaptic plasticity, rather than a change in synaptic strength itself. A physiological state that alters which circuit is recruited for learning, or how strongly a given coincidence of activity is translated into a change in synaptic weight, is metaplastic in exactly this sense — and hunger and sleep pressure, the two internal states most directly relevant to this thesis, both illustrate the point concretely.

Hunger is the more thoroughly worked out of the two. Tsao et al. (2018) showed that the MB itself, not only peripheral or hypothalamus-like feeding centers, integrates hunger and satiety signals to control food-seeking behavior in Drosophila. Flies approach yeast odor only when food-deprived, and this hunger-driven food-seeking depends on KC output and, specifically, on five MBON types whose dendrites define a subset of MB compartments. In vivo imaging showed that the odor-evoked responses of these MBONs are bidirectionally modulated by starvation, and that this modulation is implemented by six types of dopaminergic neurons innervating the same compartments, acting through the dopamine receptor DAMB expressed in both the KCs and the MBONs themselves. In other words, the same dopaminergic, compartment-restricted architecture that Section 1.2 described as the substrate for

associative learning is also the substrate through which hunger reconfigures the fly's response to food related odors: the DANs, in this case, are reporting the fly's metabolic state rather than an external unconditioned stimulus, but the circuit logic — dopamine gating the KC-to-MBON transformation within a compartment — is the same.

Sleep pressure provides a still sharper illustration, because it does not merely modulate the strength of a memory but determines which of two anatomically distinct circuits is used to consolidate it at all. Chouhan et al. (2020) trained flies on an appetitive odor-sugar association and then either fed or starved them during the post-training consolidation window. Fed flies required an increase in post-training sleep to consolidate long-term memory, and sleep depriving them abolished it; starved flies, by contrast, consolidated the same long-term memory without any requirement for post-training sleep, and sleep deprivation had no effect on their performance. This sleep-dependent/sleep-independent split is not a graded shift within one pathway but a switch between two developmentally and anatomically separate subsets of the α′/β′ Kenyon cells — an anterior-posterior subset (α′/β′ap) required for memory only in fed flies, and a medial subset (α′/β′m) required for memory only in starved flies — each recruiting its own distinct dopaminergic neurons and its own distinct MBONs. The two circuits are coupled to sleep itself in different ways, too: the MBONs required for the fed, sleep-dependent form of memory also independently promote sleep, so that the same nodes that consolidate the memory also help generate the physiological state the consolidation depends on. Which of the two circuits is engaged is itself set by a hunger signal: flies lacking the receptor for Neuropeptide F (NPF, the Drosophila ortholog of vertebrate NPY) remain dependent on sleep for memory consolidation even when starved, indicating that NPF signaling is what normally licenses the switch to the sleep-independent route under hunger.

Taken together, these two examples make the metaplasticity framing concrete rather than metaphorical. Hunger does not simply add a food-seeking bias on top of an unchanged associative circuit; it changes the gain of dopamine-gated plasticity at specific KC-MBON compartments (Tsao et al., 2018). Sleep pressure does not simply make an existing memory more or less likely to persist; acting through the

same hunger signal, it determines which anatomically and molecularly distinct plasticity pathway is recruited to store the memory in the first place (Chouhan et al., 2020). In both cases, the physiological state is read out through the same kind of dopaminergic, compartment-specific architecture already described for associative learning, but the effect of that readout is on the plasticity process itself — its gain, or its circuit of implementation — rather than on behavior directly. It is worth being precise about what kind of claim this is, because there is a difference between a state modulating an otherwise externally triggered plasticity event and a state inducing plasticity in its own right, and the two examples above only establish the former. In both Tsao et al. (2018) and Chouhan et al. (2020), the plasticity event itself is still set in motion by something external and discrete — an odor paired with sugar, an odor paired with dopamine — and hunger or sleep pressure act as a gate on whether, or through which circuit, that externally triggered event is expressed. Section 1.3, however, already supplies a reason to think the postsynaptic mechanism itself is not restricted to this kind of explicit, paired trigger. Pribbenow et al. (2022) showed that α2 nAChR dynamics at MB output synapses are engaged not only during associative training but also during non-associative familiarity learning, in which mere repeated exposure to an odor — with no explicit reinforcement, no unconditioned stimulus, no paired dopamine at all — is sufficient to induce a lasting change in α2 receptor dynamics at the corresponding synapse. If postsynaptic plasticity at these synapses can already be triggered by an experience as minimal and as unreinforced as repeated exposure, there is no principled reason to assume it could not, in principle, also be triggered by a sufficiently strong and sufficiently sustained internal signal, even one that is not tied to any single discrete external event at all.

Accumulated sleep pressure is exactly this kind of signal: an internal variable that builds up continuously with time spent awake, that is tracked and read out by dedicated elements of the MB output layer itself (Section 1.2), and that is communicated, at least in part, through the same dopaminergic and cholinergic machinery already implicated in postsynaptic plasticity elsewhere in the MB. This is what motivates treating accumulated sleep pressure not merely as a modulator that gates whether some other, externally triggered plasticity event is expressed, but as a candidate inducing signal in its own right — one capable of driving a change in the

postsynaptic receptor complement of specific MB output synapses on its own, independently of any associative training paradigm. Whether this is in fact the case, and which MB compartments and receptor subunits are involved, depends on the specific circuit through which sleep pressure is thought to act on the MB, which the remainder of this chapter now turns to.

1.5 The mushroom body sleep homeostasis: segregated microcircuits and an open question about the postsynaptic side

Sitaraman et al. (2015) provided the first functional dissection of the MB circuit responsible for homeostatic sleep regulation, using the same MBON population already introduced in Section 1.2. Behavioral epistasis experiments — combining thermogenetic activation of specific KC subtypes with synaptic silencing of specific MBONs — identified two segregated, functionally opposed microcircuits within the MB output layer. In one, *γd* KCs synaptically excite the sleep-promoting neuron MBON-γ2α′1; activating *γd* KCs increases sleep, and this effect is abolished by silencing MBON-γ2α′1. In the other, *α′/β′* and *γm* KCs excite the wake-promoting neuron MBON-γ5β′2a/β′2mp (and its bilateral counterpart); activating these KCs decreases sleep, and this effect is abolished by silencing MBON-γ5β′2a. Direct physiological connectivity mapping, pairing optogenetic KC activation with calcium imaging of the postsynaptic MBON, confirmed that *α′/β′* KCs excite MBON-γ5β′2a far more strongly than MBON-γ2α′1, and that this excitatory drive is compartmentalized rather than diffuse. Both MBON outputs converge on the same pair of downstream regions, the superior medial protocerebrum (SMP) and crepine (CRE), consistent with the two microcircuits feeding into a shared decision point rather than acting through entirely separate downstream targets.

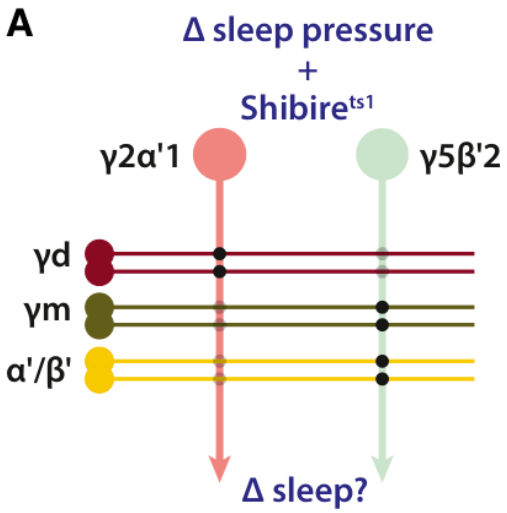


Fig. 1.4 The segregated sleep/wake microcircuit model proposed by Sitaraman et al. (2015). γd KCs excite the sleep-promoting MBON-γ2α'1; α′/β′ and γm KCs excite the wake-promoting MBON-γ5β′2a/β′2mp. Silencing either MBON (Shibirets1) while manipulating sleep pressure or KC activity tests each microcircuit's causal contribution to sleep. Adapted from Sitaraman et al. (2015).

A specific and, for this thesis, important detail of that dissection is that silencing either MBON on its own, without simultaneously activating its presynaptic KCs, had no detectable effect on sleep. Only when the relevant KC population was concurrently activated did silencing the corresponding MBON reveal a behavioral phenotype. Sitaraman et al. (2015) interpreted this as evidence that these microcircuits are relatively inactive under basal conditions — the MBONs contribute little to ongoing behavior unless their presynaptic KCs are actively driving them. This detail matters because it establishes, at baseline, that MBON output in this circuit is normally dominated by presynaptic drive rather than by some fixed, drive-independent postsynaptic tone.

Whether this remains true once sleep pressure itself, rather than an artificial optogenetic stimulus, is the source of drive was addressed directly with electrophysiology. Sitaraman et al. (2015) used the genetically encoded voltage indicator ArcLight to record spontaneous membrane electrical activity in brain explants from flies sleep-deprived for 16 hours and from non-deprived controls. Sleep deprivation increased the spontaneous electrical activity of the sleep-promoting elements of the circuit — MBON-γ2α′1 dendrites ($p < 0.01$) and *γd* KC axons ($p < 0.05$) — and decreased the activity of the wake-promoting elements — MBON-γ5β′2a/β′2mp dendrites and *α′/β′* KC axons (both $p < 0.05$) — while

leaving *γm* KC activity statistically unaffected. This double dissociation, with opposite signs in the sleep and wake-promoting arms of the circuit, was interpreted as a homeostatic scaling process: accumulating sleep pressure shifts the relative balance of activity between the two microcircuits in the direction that favors sleep. Consistent with a causal role, silencing MBON-γ2α′1, or the *γd* KCs that excite it, after sleep deprivation severely blunted the homeostatic rebound sleep that otherwise follows a night of deprivation.

Weiss and Donlea (2021) then asked whether these functional, activity-level changes are accompanied by structural changes in the corresponding synapses. Using the presynaptic active-zone marker Bruchpilot (BRP), they found that sleep deprivation broadly increases presynaptic BRP abundance within KC axons across the MB lobes — a change attributable specifically to the KCs themselves rather than to other MB-intrinsic or extrinsic cell types, and one that reverses within 48 hours of recovery sleep. When they went on to ask whether this presynaptic change translates into altered synaptic *contact* with specific postsynaptic partners, using an activity-dependent GFP reconstitution across synaptic partners (GRASP) reporter of KC-to-MBON connectivity, the picture became considerably less uniform. Sleep-deprived flies showed increased KC-to-MBON GRASP signal at the MBON-α′1 and MBON-α2sc compartments, *decreased* GRASP signal at MBON-γ5β′2a and, critically, at MBON-γ2α′1, and no significant change at several other compartments (MBON-γ4>γ1γ2, MBON-β′2mp/γ5β′2a, and MBON-γ1pedc). Sleep loss, in other words, does not scale KC output synapses uniformly; different KC-to-MBON connections are modulated independently, and in different directions, by the same manipulation.

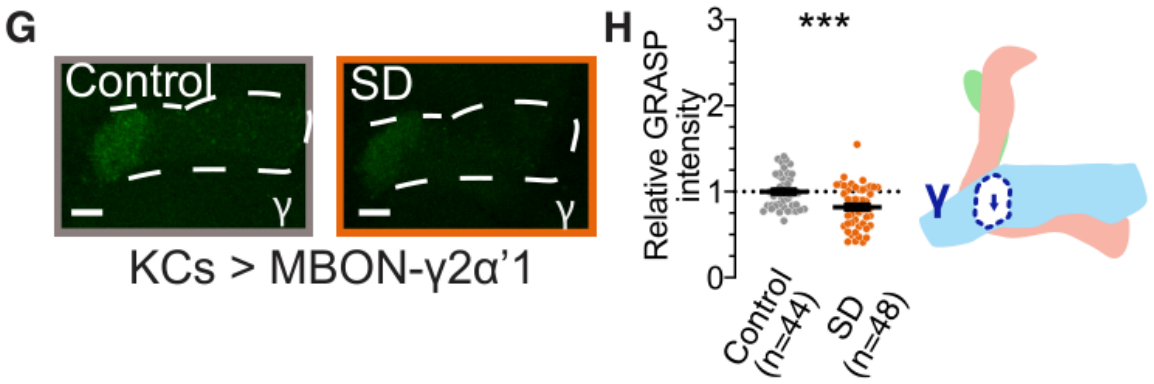


Fig. 1.5 Sleep deprivation decreases KC-to-MBON-γ2α'1 structural connectivity. Representative nsyb-GRASP images (left) and quantification of relative GRASP intensity (right) between presynaptic KCs and postsynaptic MBON-γ2α'1 in rested controls versus sleep-deprived flies (t = 3.793, p = 0.0003, n = 44–48 hemispheres/group). Adapted from Weiss and Donlea (2021), Figure 5G-H.

Read side by side, these two data sets converge on the same compartment — MBON-γ2α′1 — but appear to point in different directions. Sitaraman et al. (2015) report that sleep deprivation *increases* the spontaneous electrical activity of MBON-γ2α′1. Weiss and Donlea (2021) report that the same manipulation *decreases* the structural GRASP contact between KCs and that same MBON. If MBON activity were a simple, linear readout of how much presynaptic contact it receives, a facilitation on one measure and a reduction on the other are not easily reconciled: fewer or weaker anatomical KC contacts would, all else being equal, be expected to drive *less* postsynaptic activity, not more. This is not necessarily a contradiction between the two studies — GRASP reports the availability of active synaptic contacts, not the strength or efficacy of the ones that remain, and the two measurements were made in different preparations and with different reporters — but it is, at minimum, a pattern that a purely presynaptic account of the circuit's homeostatic scaling does not obviously explain.

This tension leaves an explicit question open, one that neither study directly answers: are these changes in the electrical activity of MBON-γ2α′1 only due to an increase in KC drive, or are there postsynaptic rearrangements induced by sleep deprivation directly? The question is sharpened by a detail already introduced above: Sitaraman et al. (2015) showed that modulating MBON activity on its own, without concurrently activating the presynaptic KCs, does not affect sleep — but this was established under baseline, non-deprived conditions, and there is no particular reason to assume the same would hold once the brain is itself sleep-deprived. If the

changes induced by sleep deprivation are occurring also at the postsynaptic level, and not only in the presynaptic KC population, then it should in principle be possible to detect a change in MBON output intensity that is independent of presynaptic plasticity — that is, a facilitation of the postsynaptic response to a given amount of presynaptic drive, rather than only a change in how much drive that presynapse provides.

Two features of the literature reviewed above motivate a specific way of resolving this. First, Sitaraman et al.'s (2015) own finding that MBON-γ2α′1 is comparatively silent unless its presynaptic KCs are actively driving it means that, ordinarily, this MBON's output is expected to track presynaptic drive fairly directly — which is exactly why a scenario in which presynaptic contact goes down while postsynaptic activity goes up is worth taking seriously rather than dismissing as noise. Second, Section 1.3 already established that MB output synapses of exactly this kind possess a genuine, non-associative postsynaptic plasticity mechanism, implemented by activity-dependent trafficking of the α2 nAChR subunit, that can operate independently of whatever is happening presynaptically. Taken together, these two facts raise a specific, testable possibility that neither Sitaraman et al. (2015) nor Weiss and Donlea (2021) directly addressed: that the increased MBON-γ2α′1 activity observed after sleep deprivation is not explained solely by presynaptic KC drive, but also reflects a change in postsynaptic receptor availability or sensitivity at that same synapse — an increase in postsynaptic α2 nAChR expression that would allow a smaller or weaker set of KC contacts to produce, if anything, a larger postsynaptic response.

This reasoning generalizes beyond MBON-γ2α′1. The same logic applies to M4/M6 and MVP2, the MBON types in which Pribbenow et al. (2022) and Pribbenow (2025) established the existence of α2- and α5-dependent postsynaptic plasticity in the context of memory (Section 1.3), but whose postsynaptic receptor complement after sleep deprivation specifically has not been examined by either Sitaraman et al. (2015) or Weiss and Donlea (2021). If postsynaptic α2 nAChR plasticity is a comparatively general property of MB output synapses — engaged by associative learning, by non-associative familiarity learning, and potentially by sleep pressure — then measuring α2 expression at these MBON postsynapses, in sleep-deprived

versus rested brains, is a direct way of asking whether the postsynaptic compartment of the MB is also a site of sleep-deprivation-induced synaptic scaling, alongside the presynaptic compartment that Weiss and Donlea (2021) characterized.

2. Aim of the Work

The work described in this thesis was carried out at Charité – Universitätsmedizin Berlin, Institute of Neurophysiology, Owald Lab.

The aim of this work is to test, directly and systematically, the postsynaptic hypothesis motivated in the preceding chapter: that sleep deprivation induces changes in α2 nAChR subunit expression at mushroom body output synapses, and that such changes contribute to the functional and structural phenotypes already reported in the literature (Sitaraman et al., 2015; Weiss and Donlea, 2021). This is pursued through three specific aims.

Aim 1: anatomically unbiased quantification. The first aim is to quantify α2-EGFP fluorescence, as a proxy for postsynaptic α2 nAChR subunit expression, across all ten mushroom body output compartments accessible with the endogenously tagged α2GFP reporter line (Section 1.2), comparing sleep-deprived flies to non-deprived controls. Surveying the full anatomical breadth of the mushroom body output layer, rather than restricting the analysis a priori to a single compartment, makes it possible to assess how widespread — or how compartment-specific — any sleep-deprivation-induced postsynaptic change actually is.

Aim 2: dissociating sleep pressure from feeding state. The second aim is to determine whether any such change is specific to sleep pressure, specific to feeding state, or reflects an interaction between the two. Hunger and sleep pressure are not independent variables at the level of MB output (Section 1.4): Tsao et al. (2018) showed that feeding state bidirectionally modulates MBON odor responses, and Chouhan et al. (2020) showed that feeding state gates which circuit, and even whether sleep itself, is required for memory consolidation. A full factorial design — comparing non-deprived controls (CNTRL) to flies that are sleep-deprived (SD), food-deprived (FD), or subjected to combined food and sleep deprivation (FDSD) — makes it possible to dissociate these possibilities directly, rather than attribute any sleep-deprivation effect to sleep pressure by default.

Aim 3: testing a priori motivated compartments. The third aim is to test three compartments motivated by the literature reviewed in Chapter 1 against specific,

directional predictions, rather than relying solely on an unbiased anatomical survey. M4/M6 and MVP2 are the MBON types in which α2, together with α5 and Dlg, mediates postsynaptic plasticity in the context of associative memory (Pribbenow et al., 2022; Pribbenow, 2025); measuring α2 expression at these same compartments under sleep and/or food deprivation — manipulations involving no training, reinforcement, or explicit odor pairing — tests whether that postsynaptic mechanism generalizes to purely homeostatic, physiological triggers. MBON-γ2α′1 is motivated directly by the tension between Sitaraman et al. (2015) and Weiss and Donlea (2021) described in Section 1.5: if the sleep-deprivation-induced increase in its electrical activity reflects, at least in part, a postsynaptic contribution rather than presynaptic drive alone, this should register as an increase in α2 expression at that compartment specifically, independently of the reduction in KC-to-MBON-γ2α′1 GRASP signal already reported.

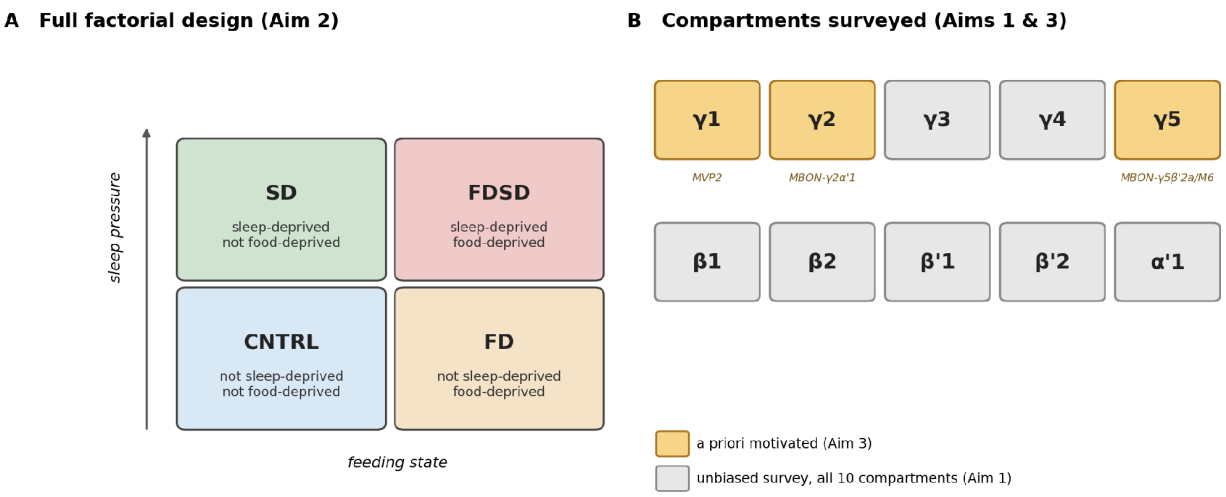


Fig. 2.1 Overview of the experimental design used to address the three aims of this work. (A) The full 2×2 factorial design, crossing sleep deprivation with food deprivation, yields four groups (CNTRL, SD, FD, FDSD), enabling Aim 2's dissociation of sleep- and hunger-driven effects. (B) All ten mushroom body output compartments accessible with the α2GFP reporter line are surveyed (Aim 1); three compartments — γ1 (MVP2), γ2 (MBON-γ2α'1), and γ5 (MBON-γ5β'2a/M6) — are additionally motivated by specific, a priori predictions from the literature reviewed in Chapter 1 (Aim 3).

Beyond resolving the specific tension between Sitaraman et al. (2015) and Weiss and Donlea (2021) at MBON-γ2α′1, these aims bear on a broader question about how invertebrate central synapses implement postsynaptic homeostatic plasticity. The clearest existing evidence for activity-dependent α2 trafficking at MB output synapses comes from associative learning paradigms, in which a specific, trained memory trace is being consolidated (Pribbenow et al., 2022; Pribbenow, 2025). Testing whether the same postsynaptic mechanism is also recruited by a purely physiological, non-associative state — sleep pressure, arising independently of any trained association — asks whether α2-dependent postsynaptic plasticity is a general-purpose property of MB output synapses, engaged whenever a sufficiently strong homeostatic demand is placed on the circuit, or whether it is instead specific to the associative-learning context in which it was first characterized.

The working prediction, grounded in the homeostatic logic of the circuit set out in Chapter 1, is that sleep deprivation increases α2 expression preferentially in sleep-promoting compartments such as MBON-γ2α′1, with comparatively little or no corresponding change in wake-promoting or purely associative-memory compartments outside the sleep-control microcircuit. Whether this effect is specific to sleep pressure, or is instead shaped by feeding state, is precisely what Aim 2 is designed to resolve. How these predictions hold up across the full set of compartments surveyed is addressed in the Results and Discussion that follow the description of the experimental methods set out in the next chapter.

3. Methods

This chapter describes the experimental procedures used to test the prediction set out in Chapter 1: whether sleep deprivation, alone or in combination with food deprivation, alters postsynaptic α2 nAChR subunit expression across mushroom body output compartments.

3.1 Fly stocks and husbandry

The α2-EGFP line, in which the endogenous α2 nAChR subunit locus is tagged with EGFP (Section 1.2), was maintained on standard cornmeal medium at 25°C. Stocks were flipped onto fresh food and new vials established on a fixed three-day cycle (Monday, Wednesday, Friday); on each of these days, newly hatched, mixed-sex progeny were collected and labelled with the collection date, to allow cohorts to be tracked across experimental rounds.

Only flies homozygous for the α2-EGFP allele were used in experiments. Homozygosity was established by screening founder flies against the dominant Tubby (Tb) marker carried on the balancer chromosome, and retaining only non-Tubby individuals to seed pure homozygous stock vials. Because these founder vials then propagated as self-sustaining homozygous stocks, routine genotyping of subsequent generations was unnecessary; manual screening was restricted to periodic spot checks confirming the continued absence of Tubby flies. Stock vials remained in use for as long as the food medium supported healthy development — typically 10–14 days after the first adults hatched — after which fresh stocks were established from the same homozygous line. For each experiment, newly hatched, mixed-sex progeny were collected and aged for 5–9 days before use; sex composition at the point of tissue collection is described in Section 3.3.

3.2 Sleep deprivation / food deprivation paradigm

The experiment followed the factorial design introduced in Section 1.5, crossing sleep deprivation with food deprivation: four groups — untreated controls (CNTRL), sleep-deprived flies (SD), food-deprived flies (FD), and flies subjected to combined food and sleep deprivation (FDSD) — were run in parallel within each experimental round, so that the effects of sleep deprivation, food deprivation, and their interaction

could be assessed independently of one another rather than confounded with the specific day or cohort tested.

For each round, 5–9-day-old, sex-mixed flies were first pooled into a single vial to randomize cohort composition across conditions, then redistributed into six smaller vials: one CNTRL vial, one FD vial, two SD vials, and two FDSD vials. The SD and FDSD groups were run in duplicate vials as a precaution against mortality associated with the sleep deprivation protocol, to guarantee a sufficient number of surviving flies for dissection. Vial allocation was carried out at a fixed time on the day before dissection (10:20–10:40 AM); this moment marked the onset of the ~20–22 h food deprivation period for the FD and FDSD groups, and served as the common time reference against which the sleep deprivation protocol and the dissection schedule were both standardized.

Following allocation, CNTRL and FD vials were transferred to a 25°C incubator and left undisturbed until dissection. SD and FDSD vials were instead placed in a custom-built mechanical sleep deprivation apparatus, programmed to begin vibrational stimulation at 8:00 PM and to continue uninterrupted until dissection the following morning; each stimulus consisted of a 1.5-s vibrational pulse delivered every 20 s (apparatus configuration: COM4 serial channel, Light Channel 2, Pulse setting 3). This schedule guaranteed SD and FDSD flies a minimum of 12 h of continuous mechanical sleep deprivation (20:00–08:00/10:00) before dissection (Figure 3.1).

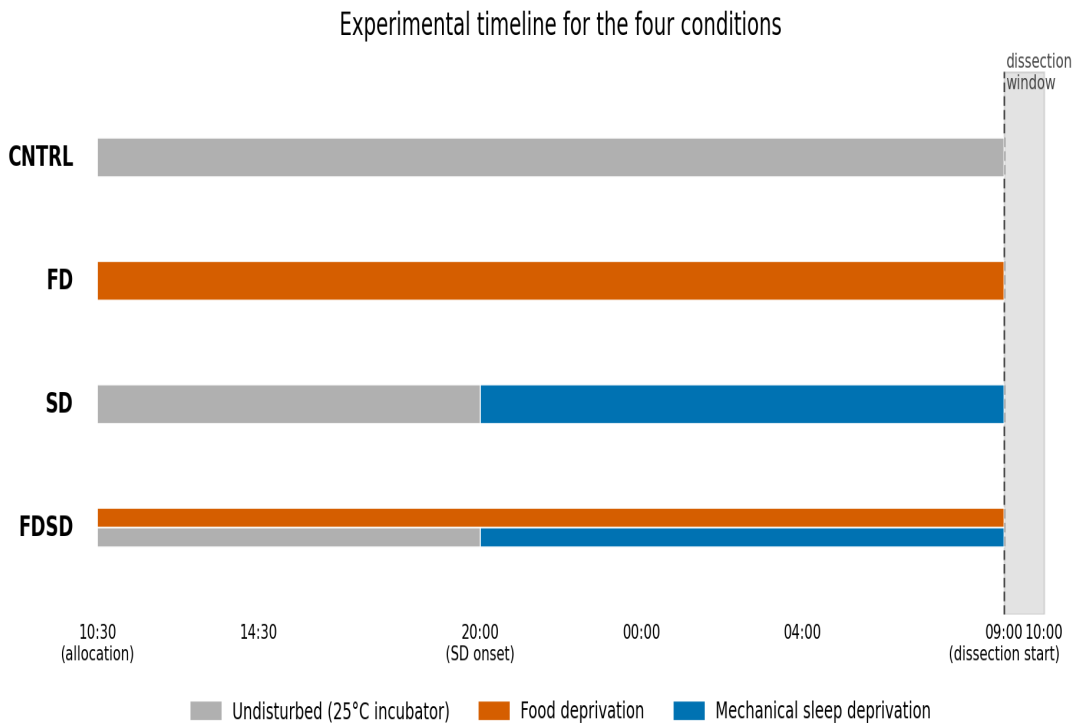


Fig. 3.1 Experimental timeline for the four conditions (CNTRL, FD, SD, FDSD). Vial allocation at 10:30 AM marks the onset of the ~20–22 h food deprivation period for FD/FDSD; mechanical sleep deprivation begins at 8:00 PM for SD/FDSD and continues, uninterrupted, until dissection the following morning (9:00–10:00 AM).

Dissections began at 9:00 AM on the day following treatment onset. The order in which the four groups were dissected was randomized across experimental rounds (Table 3.1), so that group identity would not be systematically confounded with time of dissection, while still respecting the two fixed constraints described above: a minimum of 12 h of sleep deprivation for SD and FDSD, and 20–22 h of food deprivation for FD and FDSD.

Round	Dissection order
08/05	FDSD → SD → CNTRL → FD
21/05	FD → FDSD → CNTRL → SD
17/07	SD → CNTRL → FD → FDSD
21/07	CNTRL → SD → FDSD → FD

Table 3.1 Randomized order of dissection across the four experimental rounds.

3.3 Tissue processing, confocal imaging, and ROI quantification

Prior to dissection, approximately ten female flies were selected from each experimental cohort, targeting a yield of at least five intact brains per condition. Flies were rapidly decapitated and heads immediately submerged in ice-cold phosphate-buffered saline (PBS) within a chilled dissection chamber; brains were then microdissected individually under a stereomicroscope, while undissected heads were kept in ice-cold PBS to preserve tissue integrity and fluorescence signal. Dissected brains were pooled into a single microcentrifuge tube containing ice-cold PBS until the target number for that condition was reached.

Once the quota was met, the PBS supernatant was aspirated and replaced with 200 µL of 4% paraformaldehyde (PFA) to begin fixation. Brains were fixed in 4% PFA for 20 min, briefly rinsed in PBS containing Triton X-100 (PBST), washed for 30 min in PBST, and then washed twice more for 20 min each in plain PBS. To keep pace with the randomized dissection schedule, this fixation and washing sequence for one cohort was run concurrently with the dissection of the next, so that processing time did not distort the planned order of groups.

Fixed brains were mounted on glass slides in VECTASHIELD antifade mounting medium, oriented anterior side up and aligned using the antennal lobes as landmarks to ensure consistent dorsoventral orientation and planarity for confocal access to the MBON dendritic fields. Mounted slides were stored in the dark at 4°C for at least one night before imaging, to allow the mounting medium to clear the tissue.

Confocal imaging was performed on a Leica SP8 gated STED confocal microscope (Charité NWFZ Light Microscopy Facility), using Leica Application Suite Advanced Fluorescence (LAS-AF) software and a 63× objective. EGFP was excited with a 20%-power Argon laser line, and emission was collected at 500–550 nm using a high-sensitivity hybrid detector (HyD.1) in standard EGFP detection mode. Images were acquired in xyz mode with bidirectional scanning at 2000 × 1400 px (pixel size 123.08 nm) and a frame average of 2 (no line averaging); serial optical sections were collected at 0.5 µm z-steps through the full depth of the MBON compartments, imaging both hemispheres whenever tissue integrity allowed.

Quantification was performed in Fiji/ImageJ. For each brain, ten mushroom body lobe compartments — γ1–γ5, β1–β2, β′1–β′2, and α′1 — were identified from anatomical landmarks and outlined with the freehand ROI tool (Figure 3.2). These compartments correspond to the dendritic fields of specific MBON types already discussed in Chapter 1: γ2 and γ5, in particular, correspond to the dendritic compartments of MBON-γ2α′1 and MBON-γ5β′2a/M6 respectively — the sleep- and wake-promoting nodes whose apparently conflicting presynaptic and electrophysiological profiles motivated this study (Section 1.5). Mean gray value (EGFP intensity) was measured within each ROI on five consecutive optical slices per compartment, and measurements were exported from Fiji's Measure/ROI Manager output into a single compiled dataset, with one row per slice × compartment × fly, recording fly identity (including hemisphere), experimental group, slice number, compartment, and mean gray value.

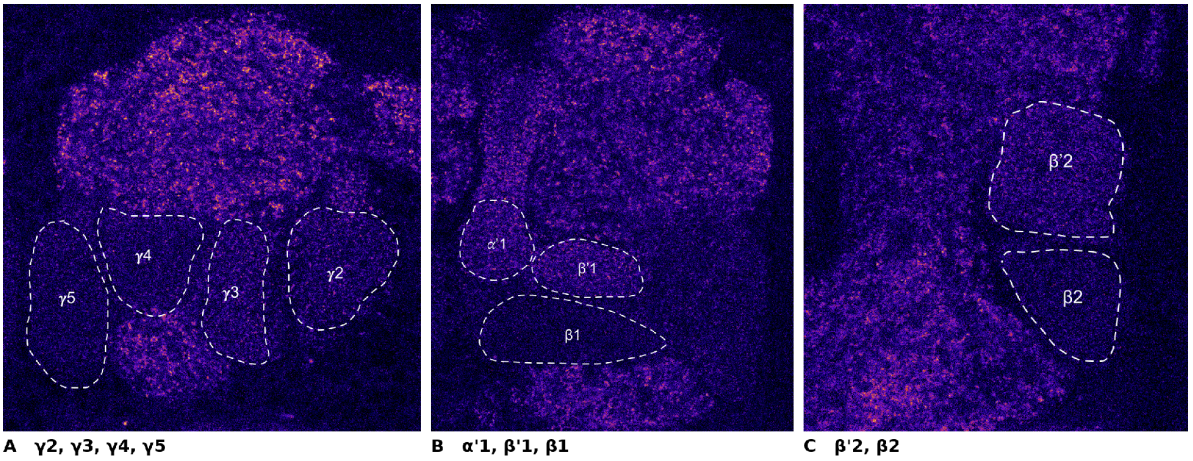


Fig. 3.2 Representative confocal images and example ROIs for nine of the ten mushroom body lobe compartments quantified in this study (γ1 not shown), outlined with the freehand ROI tool in Fiji/ImageJ. Images are displayed with a "Fire" lookup table for visualization only; quantification was performed on the raw grayscale mean intensity within each ROI. Panels show single optical slices from one representative brain (α2-EGFP); ROI shape and position were re-drawn per brain from anatomical landmarks.

3.4 Statistical analysis pipeline

The compiled dataset (5,542 rows) was first checked and cleaned: a corrupted row caused by a missing line break was repaired; a group-label typo ("CNTTRL", corrected to CNTRL) was fixed; one fly with grossly incomplete data (only 1 of ~500 expected values present) was excluded; one Fly_ID that had inadvertently been assigned to two different flies in two different groups was disambiguated; and hemisphere and batch (hatching-date/imaging-round) identifiers embedded in the Fly_ID string were parsed out into separate fields for downstream grouping.

The dataset has a three-level nested replicate structure — optical slice (technical replicate) within hemisphere within fly within group — which, left uncollapsed, would treat technical replicates as independent data points and inflate the effective sample size. Values were therefore collapsed in two sequential averaging steps: the five slice measurements were first averaged within each fly-hemisphere × compartment combination, and the resulting left- and right-hemisphere values were then averaged per fly × compartment. This yielded a single independent value per fly per compartment — the unit used in every statistical test that follows — with final sample sizes of CNTRL = 14, SD = 19, FD = 14, and FDSD = 20 flies.

Distributional assumptions were checked before choosing a test: the Shapiro-Wilk test found 36 of 40 group × compartment cells consistent with normality ($p > 0.05$), and Levene's test found unequal variance across groups in only one of the ten compartments (γ5). Given largely normal data with only isolated heteroscedasticity, Welch's ANOVA — which does not assume equal variances — was adopted as a single robust default across all compartments, rather than switching tests on a compartment-by-compartment basis.

A mixed-design ANOVA (between-subjects factor: Group; within-subject/repeated factor: Compartment; subject: fly) was run first, as an omnibus check of whether condition affected fluorescence overall and whether any such effect was uniform across compartments. The Group × Compartment interaction was significant ($F(27,567) = 1.98$, $p = 0.0026$), alongside significant main effects of Group ($F(3,63) = 3.86$, $p = 0.013$, partial $\eta^2 = 0.155$) and, expectedly, of Compartment ($F(9,567)$, $p < 0.001$, reflecting baseline differences in fluorescence intensity across zones).

Because the interaction indicated that any effect of condition was compartment-specific rather than uniform, group differences were subsequently tested separately within each of the ten compartments using Welch's ANOVA, and the resulting raw p-values were corrected for the ten compartments tested using the Benjamini-Hochberg false discovery rate (FDR) procedure.

Within each compartment, Dunnett's test was then used to compare each treatment condition (SD, FD, FDSD) against CNTRL specifically, within a single corrected family of three comparisons. Dunnett's test was preferred over a full pairwise approach (e.g., Tukey's or Games-Howell) because the comparisons of biological interest were restricted to a shared reference group, for which Dunnett's test offers greater statistical power than a full pairwise correction.

All analyses were carried out in Python, using pandas for data handling, scipy.stats for the Shapiro-Wilk, Levene's, and Dunnett's tests, pingouin for the mixed-design and Welch ANOVAs, and statsmodels for the Benjamini-Hochberg FDR correction. Claude was used as an AI coding assistant during the development of the analysis scripts, including drafting and troubleshooting the Python code implementing the pipeline described above; all statistical choices, test selection, and interpretation of the results remained the responsibility of the author.

4. Results

4.1 Sleep deprivation increases postsynaptic α2 expression in a subset of mushroom body compartments

The omnibus mixed-design ANOVA reported in Section 3.4 indicated a significant main effect of Group ($F(3,63) = 3.86$, $p = 0.013$) and, critically, a significant Group × Compartment interaction ($F(27,567) = 1.98$, $p = 0.0026$), showing that the effect of condition on α2-EGFP expression was not uniform across the mushroom body but concentrated in specific compartments. Group differences were therefore examined separately within each of the ten compartments sampled (Figure 4.1).

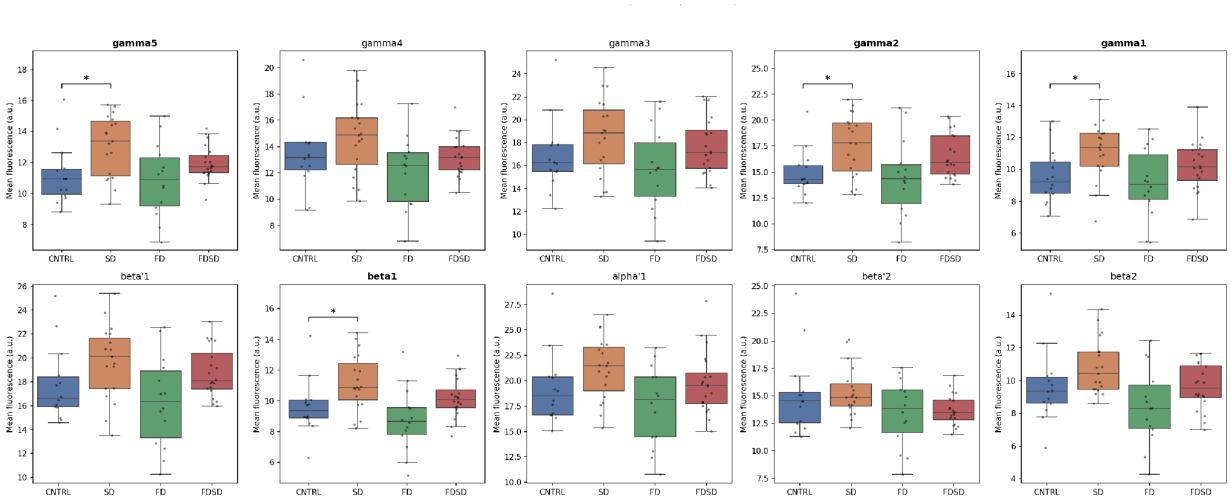


*Fig. 4.1. α2-EGFP fluorescence intensity per mushroom body compartment, by condition (animal-level, n = 1 value/animal/ROI). Boxes show median and interquartile range; individual points are single flies. Brackets mark significant Dunnett's post-hoc comparisons against CNTRL (*p < 0.05); compartments with a significant omnibus effect are bolded.*

Of the ten compartments tested, four showed a significant increase in α2-EGFP fluorescence in sleep-deprived (SD) flies relative to non-deprived controls (CNTRL) by Dunnett's test: γ5 ($p = 0.016$), γ2 ($p = 0.021$), γ1, and β1 (both $p < 0.05$) (Figure 4.2). In none of the ten compartments did food-deprived (FD) or combined food- and sleep-deprived (FDSD) flies differ significantly from CNTRL. The remaining six compartments — γ3, γ4, β′1, α′1, β′2, and β2 — showed no significant difference between any condition and CNTRL; at the γ5-adjacent β′2 compartment specifically, the SD-CNTRL comparison was far from significance (Dunnett $p = 0.975$). γ2 and γ5 correspond to the dendritic compartments of MBON-γ2α′1 and MBON-γ5β′2a/M6

respectively (Section 3.3), the two nodes motivated in Section 1.5; γ1 corresponds to the dendritic field of MVP2, the third a priori motivated MBON type, though no directional prediction had been made for it specifically. β1 falls outside all three MBON types motivated in Section 1.5. Interpretation of these patterns, including the γ2 and γ5 findings in relation to Sitaraman et al. (2015) and Weiss and Donlea (2021), the γ1/MVP2 result in relation to a computational model of postsynaptic gain, and the absence of any FD or FDSD effect, is taken up in the Discussion.

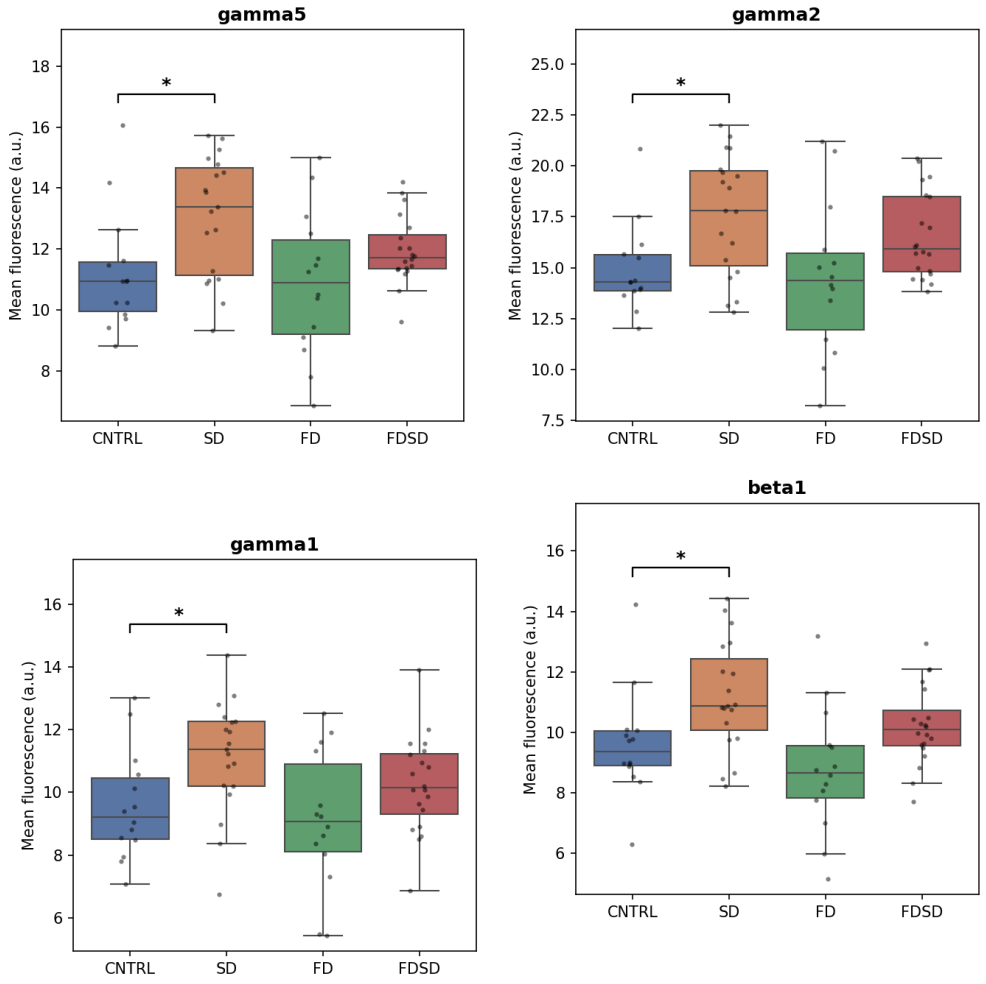


Fig. 4.2 The four compartments reaching significance by Dunnett's test (SD vs CNTRL), shown at larger scale for visual clarity.

5. Discussion

5.1 A local feedback hypothesis linking presynaptic contact loss to postsynaptic α2 upregulation

The two compartments most directly tied to the open question set out in Section 1.5 — γ2 and γ5, corresponding to the dendritic fields of MBON-γ2α′1 and MBON-γ5β′2a/M6 respectively — both show a significant, sleep-deprivation-specific increase in α2-EGFP fluorescence (Section 4.1). This is, on the face of it, a satisfying outcome: both of the compartments singled out in advance because of the tension between Sitaraman et al. (2015) and Weiss and Donlea (2021) turn out to carry a postsynaptic signature of sleep deprivation, at a location that neither of those two studies examined directly. But treating the two results as a single, uniform confirmation of the postsynaptic hypothesis would understate what is actually going on. Read against the specific circuit role of each node, γ2 and γ5 are not equally expected results: one fits a textbook homeostatic-scaling account rather directly, and the other does not, and the difference between them is itself informative.

At MBON-γ2α′1, the result is in line with classical postsynaptic homeostatic synaptic scaling. Weiss and Donlea (2021) reported that sleep deprivation reduces KC-to-MBON-γ2α′1 GRASP contacts at this compartment, and Sitaraman et al. (2015) reported that the same manipulation increases MBON-γ2α′1's spontaneous electrical activity — a pattern that, on its own, is difficult to reconcile with a purely presynaptic account of the circuit's homeostatic scaling (Section 1.5). An increase in postsynaptic α2 nAChR density is exactly the kind of change homeostatic scaling predicts under reduced synaptic drive: in the founding demonstration of this phenomenon, cortical neurons chronically deprived of activity scale up the postsynaptic strength of their remaining synapses, preserving firing output in the face of reduced input (Turrigiano et al., 1998). The logic transfers directly to a cholinergic synapse of the kind studied here: for a fixed amount of acetylcholine released per KC spike, a synapse with more postsynaptic α2 receptors converts that release into a larger depolarization, so that even a KC input that has lost some of its physical contact points can still drive as much, or more, postsynaptic current than before. This is also the same logic already introduced in Section 1.3 as the analogy between

α5/α2 and NMDA/AMPA receptors: α2 was framed there as the subunit most directly responsible for the expression, rather than the induction, of a change in synaptic weight. Framed this way, γ2's result is the straightforward case: fewer presynaptic contacts, more postsynaptic receptor, and a net increase in activity that is no longer paradoxical but is instead exactly what a homeostatically scaling synapse, expressing that scaling through its α2 complement, is expected to do.

At MBON-γ5β′2a/M6, the same logic runs the other way, and the result is the more surprising of the two. This node is wake-promoting, and Sitaraman et al. (2015) reported that its electrical activity decreases after sleep deprivation, consistent with the homeostatic shift away from wake-promoting output that accompanies rising sleep pressure. If postsynaptic α2 density were simply tracking this node's activity trajectory — or being scaled to preserve a wake-promoting drive that the circuit is actively working to suppress — the more intuitive prediction would have been a decrease in excitatory postsynaptic receptor density at γ5, not an increase: fewer α2 receptors, a smaller postsynaptic response to whatever KC input remains, and an electrophysiological readout that decreases for two reasons at once rather than one. Instead, γ5 shows the same direction of change as γ2: more α2, not less, in a compartment whose net output is simultaneously going down. This is not easily dismissed as a nonspecific consequence of sleep deprivation on the tissue as a whole — six of the ten compartments sampled, including several that are neither sleep- nor wake-promoting, showed no change at all (Section 4.1), so whatever is happening at γ5 is compartment-specific rather than a generic stress or health effect of the deprivation protocol. Excitatory receptor upregulation in a node whose activity is being actively suppressed is, at face value, in real tension with a simple activity-matching account of homeostatic scaling, in which postsynaptic strength is adjusted to track, rather than oppose, the direction a circuit is being pushed.

One way to resolve this tension is to relocate the homeostatic response from the level of the circuit to the level of the individual synapse. Rather than treating α2 upregulation as being scaled to match each MBON's activity trajectory or behavioral role — e.g. sleep promoting or wake promoting — the two results are equally well described by a single, simpler rule operating locally at each compartment: a loss of presynaptic KC contacts (GRASP) triggers a compensatory increase in postsynaptic

α2 density, independently of whether that compartment is sleep-promoting or wake-promoting and independently of what the net behavioral consequence turns out to be. Under this account, γ2 and γ5 are not different in kind; both lose presynaptic contacts after sleep deprivation (Weiss and Donlea, 2021), and both respond with the same local postsynaptic adjustment. What differs between them is only whether that local adjustment is sufficient to shift the compartment's net output: at γ2, the postsynaptic increase coincides with a net increase in activity; at γ5, the same postsynaptic increase is engaged, but is not sufficient to prevent the net decrease in activity that the wake-suppressing arm of the circuit is otherwise driving (Figure 5.1).

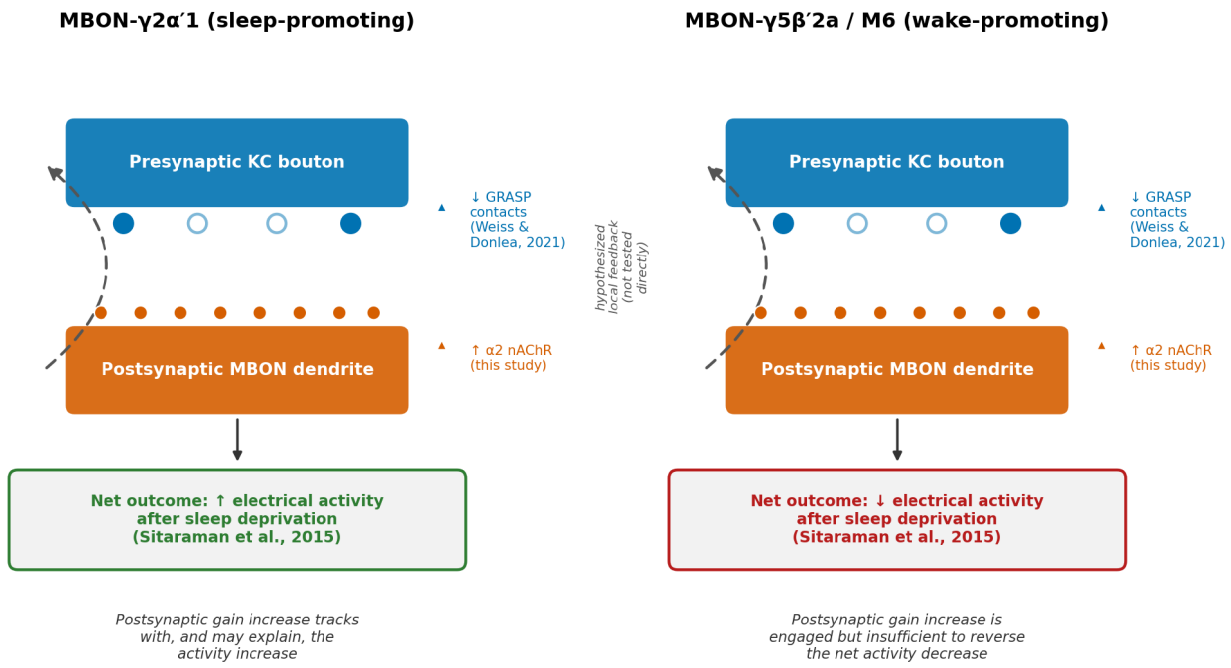


Fig. 5.1 A hypothesized local feedback loop linking presynaptic contact loss to postsynaptic α2 upregulation at KC-to-MBON synapses. At both MBON-γ2α'1 and MBON-γ5β'2a/M6, sleep deprivation reduces KC-to-MBON GRASP contacts (Weiss and Donlea, 2021) and increases postsynaptic α2-EGFP fluorescence (this study). The same local pattern coincides with divergent net outcomes: an activity increase at the sleep-promoting node, and an insufficient-to-reverse activity decrease at the wake-promoting node (Sitaraman et al., 2015). The feedback loop itself — the arrow linking reduced GRASP contact to increased α2 density — is a hypothesis motivated by this co-occurrence and is not tested directly in this study.

This kind of local, structural homeostatic response — postsynaptic receptor density compensating for a loss of presynaptic contact area, independently of the surrounding circuit's functional demands — has a long precedent in the broader

homeostatic plasticity literature, where synapse-autonomous scaling rules of this kind are well documented as a general principle of how neurons stabilize their function under perturbation (Davis, 2006). It is also, on reflection, the more plausible of the two possible designs to begin with. The original description of synaptic scaling proposed a cell-wide rule, in which a neuron scales all of its synapses by a common multiplicative factor in response to its own activity (Turrigiano et al., 1998); but subsequent work has shown that homeostatic scaling can instead be implemented synapse-by-synapse, so that individual synapses on the same neuron are adjusted independently of one another rather than in lockstep (Béïque et al., 2011). The present dataset offers its own, independent piece of evidence for exactly this kind of local specificity, and at exactly the node in question: γ5 and β′2 are the two dendritic zones of the same MBON-γ5β′2a neuron, sampled from the same brains under the same manipulation, yet only γ5 shows a significant increase in α2 while β′2 does not (Dunnett $p = 0.975$; Section 4.1). If α2 upregulation after sleep deprivation were a whole-cell property of MBON-γ5β′2a, both of its dendritic zones should have shown it; that only one does is consistent with a rule that operates locally, compartment by compartment, tracking local presynaptic contact loss rather than the neuron's activity as a whole.

It is also worth being precise about what this local, synapse-autonomous account can and cannot explain at γ5. It offers a qualitative resolution of the puzzle raised above — postsynaptic α2 upregulation occurring at a node whose net electrical activity nonetheless decreases — but it does not, on its own, offer a quantitative one, and the two should not be conflated. Later in this chapter, a computational model of postsynaptic gain at γ5 is used to ask a sharper, quantitative version of the same question: given a physiologically plausible gain function, is the observed increase in α2 density actually able to account for the magnitude of the activity decrease reported by Sitaraman et al. (2015), treating γ5 as an otherwise isolated compartment? As will be shown, it is not — the measured α2 increase alone predicts a shift in gain that is directionally difficult to reconcile with a net decrease in activity, rather than merely an insufficient brake on one. This quantitative shortfall is what motivates the addition, in that model, of a further source of inhibitory modulation onto γ5, plausibly supplied by MVP2, the third a priori motivated MBON type introduced in Section 1.5. The local feedback account developed here should therefore be read as

establishing the presynaptic-to-postsynaptic link at γ5 — the observation that reduced GRASP contact and increased α2 density co-occur at this compartment, just as they do at γ2 — rather than as a complete, self-contained explanation of γ5's net activity change; the latter requires an additional circuit element, and is taken up quantitatively later in this chapter.

It is important to be explicit about the overall status of this proposal: it is a model of covariation, not a demonstration of causation. The GRASP measurements come from an independent dataset (Weiss and Donlea, 2021) collected in different animals from the α2-EGFP measurements reported here, under the same sleep deprivation protocol; the two are consistent with one another at the level of compartment identity and direction of effect, but no experiment in this thesis directly manipulated GRASP contact number and measured the resulting change in α2 density in the same brains, nor is any specific molecular link between the two proposed. The feedback loop drawn in Figure 5.1 is therefore best read as a working hypothesis that organizes the existing pattern of results into a single rule, rather than as mechanistic evidence for a specific signaling pathway connecting presynaptic contact loss to postsynaptic receptor trafficking. Testing it directly would require measurements that the present design does not provide: tracking both GRASP contact number and α2 density in the same animals, ideally across the time course of sleep deprivation and subsequent recovery sleep, to establish whether the two changes co-occur within individual flies and not just across independent datasets; or manipulating one side of the proposed loop directly — for instance, genetically increasing or decreasing KC-to-MBON contact number at a single compartment — and asking whether α2 density at that same compartment responds accordingly.

5.2 Hunger state gates the postsynaptic response to sleep deprivation

The factorial design was built, in part, to answer a question raised in Section 1.4 and formalized as Aim 2 in Chapter 2: whether any postsynaptic effect of sleep deprivation is specific to sleep pressure, specific to feeding state, or reflects an interaction between the two. The results reported in Section 4.1 answer this question, but not in the way a simple additive model would predict. Food deprivation on its own (FD) produced no significant change in α2-EGFP fluorescence at any of the ten compartments sampled — the expected outcome if the postsynaptic mechanism under study is sleep-specific, exactly as Chapter 1 predicted. What was not predicted is what happened when food deprivation was combined with sleep deprivation. Sleep deprivation alone (SD) produced a significant increase at four compartments — γ5, γ2, γ1, and β1 — relative to CNTRL. The same sleep deprivation protocol, applied to flies that were simultaneously food-deprived (FDSD), produced a significant increase at none of them. Food deprivation did not simply fail to add its own effect; it appears to have removed an effect that sleep deprivation reliably produces on its own.

This is worth stating precisely, because it is a different claim from a null main effect of the feeding state. A null main effect would mean hunger does nothing to α2 expression, in any condition — and that is indeed what the FD-versus-CNTRL comparison shows. What the FDSD-versus-CNTRL comparison shows is a null result under a manipulation that, on its sleep-deprivation component alone, is not null. The interaction is the finding: feeding state did not add to or subtract from a fixed sleep-deprivation effect, it appears to have gated whether that effect was expressed at all. It is also a strikingly consistent finding across compartments — all four of the compartments that respond to SD alone lose that response when food deprivation is added, rather than losing it at one compartment and retaining it at another. A coincidence affecting four independent compartments in the same direction is less parsimonious than a single upstream gate acting on whatever these four compartments have in common with each other.

A first possibility to rule out is that this is simply a power artifact — that the FDSD group is underpowered relative to SD, and the difference between a significant and a

non-significant Dunnett comparison reflects sample size rather than biology. The group sizes argue against this directly: FDSD is the largest of the four groups (n = 20), larger than SD itself (n = 19; Section 3.4). If anything, the FDSD comparison entered the analysis better powered than the SD comparison that did reach significance. The absence of an effect in FDSD is not naturally explained by a shortage of flies.

One possible reading of this pattern is that food deprivation actively drives α2 expression in the opposite direction from sleep deprivation, at exactly the same compartments, so that the two effects cancel when combined. Nothing in the FD-alone data supports this reading: FD alone does not move α2 expression downward at γ5, γ2, γ1, or β1, or anywhere else — it does nothing detectable at any compartment. An active, opposing postsynaptic effect of hunger that only appears when sleep deprivation is also present, and that is otherwise invisible on its own, is possible in principle, but it is a considerably more elaborate explanation than the alternative developed below: that hunger does not oppose the sleep-deprivation effect so much as prevent it from being generated, or from being registered as a signal the postsynaptic mechanism responds to, in the first place. This is a gating account rather than an active-compensation account, and it has real precedent in the literature on hunger-sleep interactions in *Drosophila*.

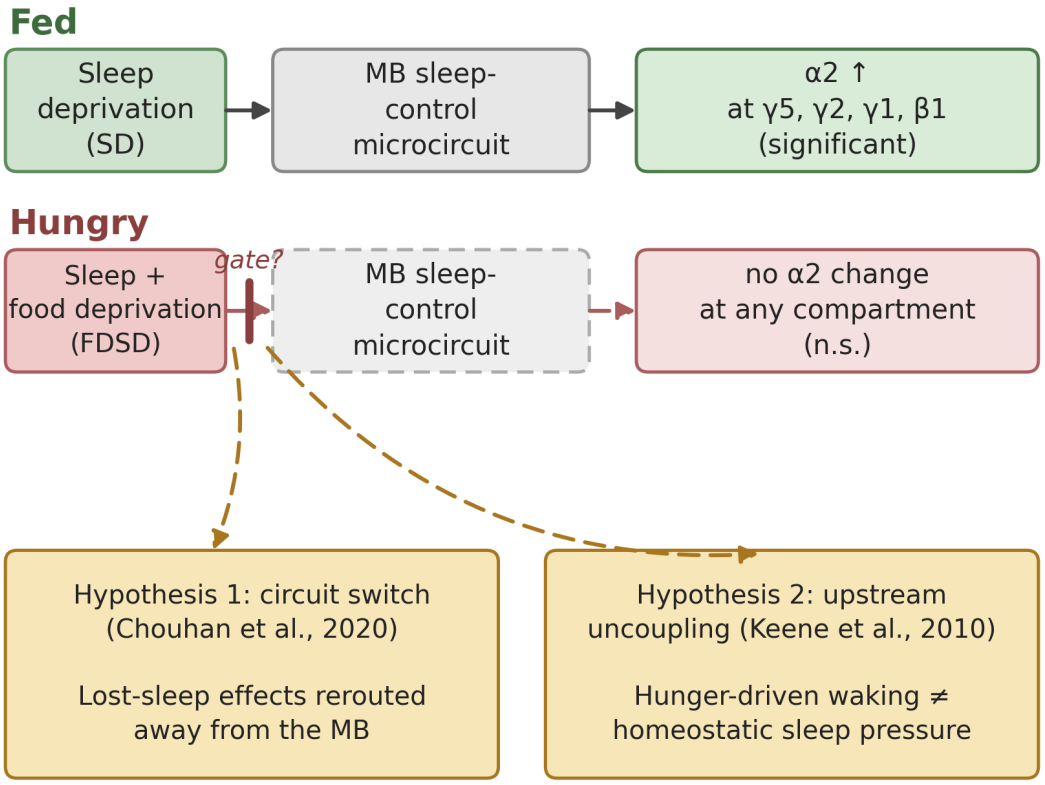


Fig. 5.2 Hunger appears to gate, rather than add to or subtract from, the postsynaptic response to sleep deprivation. In fed flies, sleep deprivation (SD) drives a significant α2 increase at γ5, γ2, γ1, and β1 via the MB sleep-control microcircuit. In hungry flies, the same sleep deprivation protocol (FDSD) produces no significant change at any compartment. Two non-mutually-exclusive hypotheses, both grounded in established Drosophila hunger-sleep circuitry but not tested directly here, are considered: a circuit switch that reroutes the consequences of lost sleep away from the MB (Chouhan et al., 2020), and an upstream uncoupling of hunger-driven wakefulness from classic homeostatic sleep-pressure signaling (Keene et al., 2010).

The clearest precedent is Chouhan et al.'s (2020) demonstration, already introduced in Section 1.4, that feeding state determines which circuit implements memory consolidation: fed flies require sleep to consolidate appetitive memory through a sleep-dependent mechanism, while starved flies consolidate the same memory without needing sleep, through a distinct, sleep-independent route. The authors interpret this as an adaptive circuit switch — an organism that is starved cannot afford to spend the time asleep that sleep-dependent consolidation would normally require, so hunger reroutes the process through a pathway that does not have that requirement. If the same kind of state-dependent rerouting generalizes from memory consolidation specifically to the broader postsynaptic scaling response measured in this thesis, food deprivation would not need to suppress the physiological consequences of lost sleep at all; it would only need to shift how those consequences are handled, away from the postsynaptic α2 upregulation at

MBON-γ2α′1, MBON-γ5β′2a/M6, and the other compartments sampled here, and toward some other, hunger-appropriate mechanism that this experiment was not designed to detect.

A second, complementary precedent operates further upstream, at the level of the sleep-pressure signal itself rather than at the level of which circuit reads it out. Starvation is well established to actively suppress sleep in *Drosophila*, producing pronounced waking and hyperactivity (Keene et al., 2010). Critically, Keene et al. (2010) also showed that this starvation-induced sleep loss does not behave like ordinary sleep deprivation in one important respect: it is not followed by the compensatory rebound sleep that normally tracks accumulated sleep pressure, and it depends on the circadian clock genes *Clock* and *cycle* acting in a specific, dorsally located clock-neuron population — a circuit the authors show is independent of the mushroom body, the canonical sleep locus targeted by Sitaraman et al. (2015) and by this thesis. If hours spent awake because of hunger are not registered by the same homeostatic-pressure signal that accumulates during ordinary mechanical sleep deprivation — or are registered predominantly through this MB-independent clock-neuron route rather than through the γd/α′/β′ microcircuit this thesis targets — then an FDSD fly could be behaviorally just as sleep-deprived as an SD fly while nonetheless failing to accumulate the specific homeostatic signal that the postsynaptic α2 response, as characterized here, is downstream of. Sleep loss, on this account, is not one uniform currency; how much of it registers as classic homeostatic sleep pressure may itself depend on why the fly is awake.

A candidate molecular link between these two levels — circuit rerouting and upstream signal suppression — is Neuropeptide F (NPF), a hunger signal that independently promotes both feeding and wakefulness in *Drosophila* (Chung et al., 2017). Flies lacking functional NPF signaling fail to suppress sleep after starvation, indicating that NPF is not merely correlated with the hungry, wakeful state but is required to produce it. NPF or a related hunger signal acting directly on the sleep-control microcircuit, or on the KC-to-MBON synapses within it, would offer a concrete point of intersection between the hunger and sleep-homeostat pathways, rather than requiring them to be wholly separate systems that merely compete for the fly's behavioral output. This remains a specific, testable proposal rather than a

demonstrated mechanism in the present system: neither Chung et al. (2017) nor any of the sleep-homeostat literature reviewed in Chapter 1 examined NPF signaling at MBON-γ2α′1, MBON-γ5β′2a/M6, or the other compartments sampled here.

These two accounts — a Chouhan-style circuit switch that reroutes the consequences of lost sleep away from the MB postsynaptic mechanism entirely, and a Keene-style upstream uncoupling of hours-awake from homeostatic sleep-pressure signaling itself — are not mutually exclusive, and the present data cannot distinguish between them, nor rule out some combination of the two together with an NPF-mediated point of contact. Both are more parsimonious than an active compensatory mechanism for the reasons already given, and both are grounded in effects that have been directly demonstrated in *Drosophila*, even though neither has previously been tested against postsynaptic nAChR expression in the MB output layer specifically. To the author's knowledge, no published study has combined sleep deprivation with food deprivation while measuring a postsynaptic marker at these compartments, which makes the FDSD null result reported here a new empirical observation rather than a replication of an already-anticipated interaction — one that existing hunger-sleep circuitry offers a plausible, but not yet directly tested, explanation for.

Distinguishing between these possibilities would require measurements beyond the scope of the present design. Quantifying total sleep loss and its time course directly in FDSD flies, rather than assuming it matches SD flies simply because the same mechanical protocol was applied, would establish whether the two groups are in fact comparably sleep-deprived at the behavioral level — a precondition for concluding that the postsynaptic difference between them reflects gating rather than a difference in the manipulation's efficacy under hunger. Manipulating NPF signaling specifically, while holding the sleep and food deprivation protocols fixed, would test whether the hunger-driven suppression of the postsynaptic response depends on this specific hunger signal or persists independently of it. And extending the anatomical survey to compartments and circuits outside the sleep-control microcircuit characterized here — including, potentially, the clock-neuron population implicated by Keene et al. (2010) — would test the circuit-switch account directly, by asking whether the

physiological consequences of lost sleep in FDSD flies are in fact being expressed somewhere else in the brain rather than nowhere at all.

5.3 A quantitative gain-modulation model, and the MVP2 inhibitory-tone hypothesis

Section 5.1 left the γ5 case as a qualitative resolution only: postsynaptic α2 upregulation at MBON-γ5β′2a/M6 is consistent, in direction, with a local feedback response to reduced presynaptic contact, but nothing in that account establishes whether the *size* of the observed α2 change is actually compatible with the size of the activity decrease that Sitaraman et al. (2015) reported at the same node. Left as a purely verbal argument, the claim that this postsynaptic increase reflects "a compensatory response that did not reach the threshold needed to reverse the net activity decrease" is a plausible-sounding story, but it is still only a story: it could just as easily be wrong, and no amount of additional qualitative reasoning can settle whether it is. Seeing a clear α2 increase at γ5 sit alongside a documented decrease in this node's electrical activity was, on its own, enough to raise real doubt about whether the two are actually compatible — doubt that only a quantitative check, rather than a further verbal argument, could resolve. This section reports that check: a minimal computational model built specifically to ask whether published presynaptic and activity data, combined with the α2 data reported in this thesis, can be reconciled under a single, shared postsynaptic mechanism, and what has to be added to make them fit.

A note on how this model was developed: the underlying idea, the hypothesis that a shared postsynaptic mechanism might reconcile the presynaptic and activity data, and the initial rough construction of the model were entirely my own. The formal description presented in this section — the explicit equation structure, notation, and derivation below — was developed with the assistance of Claude, an AI language model (Anthropic), which I used as a tool to help formalize and clearly articulate a model that I had already conceived and built.

5.3.1 Data sources and a first, important limitation

The model draws on three measurements at the same or homologous MBON nodes, each from a different source. Postsynaptic α2-EGFP fluorescence is this thesis's own data (Section 4.1, Dunnett's test values). Presynaptic KC-to-MBON contact density (GRASP) is taken from Weiss and Donlea (2021), Figure 5F (M6/γ5β′2a) and 5H

(γ2α′1). Spontaneous electrical activity (ArcLight) is taken from Sitaraman et al. (2015), Figure 5C (γ2α′1) and 5G (M6/γ5β′2a). Neither published study makes its underlying numeric values available in the main text or supplementary material; the GRASP and ArcLight values used here were read directly off the published bar-chart figures rather than obtained from an official dataset. This is one of the model's most important limitations, stated plainly at the outset rather than left implicit: the presynaptic and activity inputs to the model are approximate, figure-derived quantities, not the exact values the original authors worked with.

A second, related limitation is that the three measurements were never made together. They come from three different studies, conducted by different research groups, in different laboratories, in different years, using different transgenic reporters and different animals. The model necessarily treats them as compatible fractional-change estimates for the same underlying nodes — a working assumption, not an established fact. Both limitations are revisited in Section 5.3.6; they are noted here because they bound how the entire exercise that follows should be read: as a test of internal quantitative consistency given the best available approximations, not as an analysis of an internally consistent, jointly collected dataset.

Node	GRASP (ctrl → SD)	α2-EGFP (ctrl → SD)	Δgrasp	Δα2	Δactivity (obs.)
M6 / γ5β′2a	1.00 → 0.73	11.224 → 13.081	−27.0%	+16.5%	−53.8%
γ2α′1	1.00 → 0.83	14.927 → 17.622	−17.0%	+18.1%	+127.3%
MVP2 / γ1pedc	1.00 → 1.00 (n.s.)	9.564 → 11.130	0.0%	+16.4%	n/a

Table 5.1 The raw fractional changes (control → SD) feeding the model, for each of the three nodes considered. GRASP and α2-EGFP columns show the values themselves; Δgrasp, Δα2, and Δactivity (obs.) are the fractional changes computed from them (equations 3 and 5). No ArcLight measurement exists for MVP2/γ1pedc.

5.3.2 Model structure

Each MBON node *i* is modeled as the product of up to three multiplicative gain terms, each normalized to 1 at baseline (non-deprived control):

$$A_i(s) = D_i(s) \cdot G_i(s) \cdot I_i(s) \quad (1)$$

where $s \in [0, 1]$ is the sleep-deprivation level (0 = rested control, 1 = the full overnight sleep deprivation applied experimentally) and $A_i(s)$ is node *i*'s activity

relative to its own control. The presynaptic drive term *D* is set directly by the published GRASP data:

$$D_i(s) = 1 + \Delta\text{grasp}_i \cdot s \quad (2)$$

with Δgrasp*i* the fractional change in GRASP signal between control and full SD at node *i*, taken directly from Weiss and Donlea (2021):

$$\Delta\text{grasp}_i = (\text{GRASP}_{SD,i} / \text{GRASP}_{ctrl,i}) - 1 \quad (3)$$

The postsynaptic gain term *G* is set by this thesis's own α2-EGFP data, scaled by a single coupling constant *k* shared across *every* node:

$$G_i(s) = 1 + k \cdot \Delta\alpha2_i \cdot s \quad (4)$$

with Δα2*i* defined analogously from this thesis's own measurements:

$$\Delta\alpha2_i = (\alpha2_{SD,i} / \alpha2_{ctrl,i}) - 1 \quad (5)$$

Using one shared *k* for every node, rather than fitting a separate value at each compartment, is the model's central hypothesis: that α2 upregulation is the same molecular mechanism operating uniformly across MBON compartments, and that the divergent behavioral outcomes at different nodes arise from differences in presynaptic and circuit context, not from node-specific differences in the α2 mechanism itself. Finally, an inhibitory term *I*, defined only where relevant, captures feed-forward inhibition from MVP2 onto a target node:

$$I_i(s) = 1 - m_i \cdot s \quad (6)$$

with *mi* the fractional suppression of node *i*'s output attributable to MVP2 at full sleep deprivation. Among the nodes considered here, this term is only needed for M6/γ5β′2a; for γ2α′1 and for MVP2/γ1pedc itself, $I_i(s) = 1$.

5.3.3 Fitting the model: where a purely local account fails, and what fixes it

The coupling constant *k* is fit from γ2α′1 alone, because this node carries no inhibitory term, so equation (1) reduces to $A = D \cdot G$, solvable directly for *k* given the observed GRASP change, the observed α2 change, and the activity change Sitaraman et al. (2015) reported at this node:

$$k = [\,(1 + \Delta\text{activity}_{obs,\gamma2}) / (1 + \Delta\text{grasp}_{\gamma2}) - 1\,] / \Delta\alpha2_{\gamma2} \quad (7)$$

Substituting the γ2α′1 values from Table 5.1 (Δgrasp = −17.0%, Δα2 = +18.1%, $\Delta\text{activity}_{obs}$ = +127.3%) gives $k \approx 9.63$ — the only free parameter fit against activity

data anywhere in the model. It is then held fixed and reused, unchanged, for every other node.

Applying this same *k* to M6/γ5β′2a, using only the presynaptic and postsynaptic terms (equations 2–5, with *I* = *1*), is where the purely local account breaks down quantitatively. Given the GRASP decrease at this node (−27.0%) and the measured α2 increase (+16.5%), the model predicts a net activity *increase* of about +89% at full sleep deprivation. Sitaraman et al. (2015) instead reported a net *decrease* of −53.8% at this same node. These are not close: the model, using only the mechanism established at γ2α′1, predicts the wrong direction of change entirely at γ5. Given the α2 and GRASP data as measured, and assuming they are combinable in the way this model assumes, a purely local, two-term account is not just insufficient at M6/γ5β′2a — it is quantitatively incompatible with the observed result.

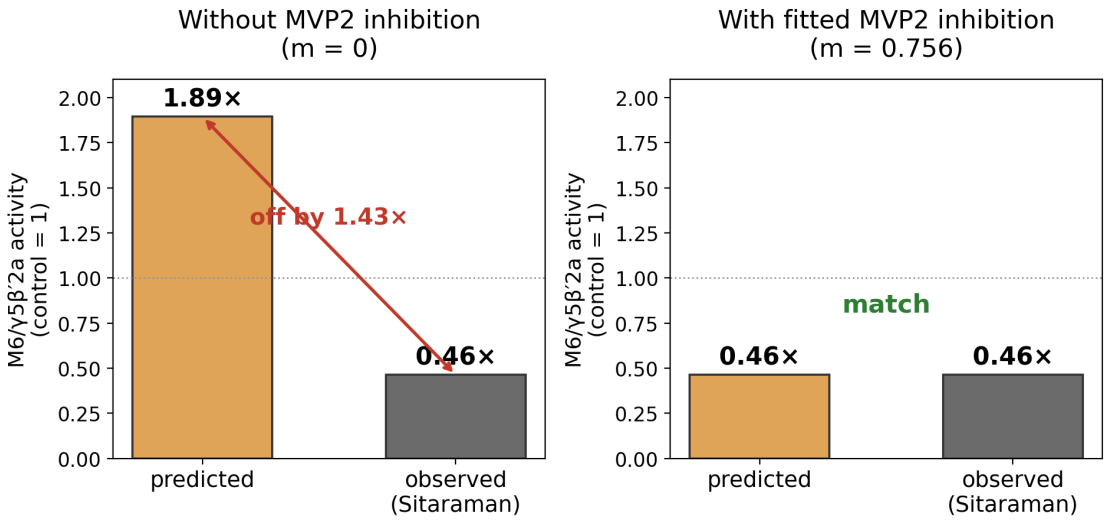


Fig. 5.3 The two-term model (presynaptic × postsynaptic gain only) predicts a 1.89-fold activity increase at M6/γ5β′2a, against an observed 0.46-fold decrease (Sitaraman et al., 2015) — a mismatch, not merely a shortfall. Adding a fitted MVP2 inhibitory term (m = 0.756) resolves the discrepancy by construction.

This mismatch is what motivates adding the inhibitory term *I* (equation 6) specifically at this node — not because independent evidence pointed to MVP2 beforehand, but because the shared-*k* model fails at M6/γ5β′2a without some additional term, and MVP2 is the most plausible anatomical candidate available, given its established feed-forward inhibitory projection onto the M4/M6 group of MBONs, which includes M6/γ5β′2a (Perisse et al., 2016). Solving equation (1) for *m* at *s* = *1* so that the model reproduces the observed activity change gives:

$$mM6 = 1 - (1 + \Delta activity_{obs,M6}) / [\,(1 + \Delta graspM6) \cdot (1 + k \cdot \Delta\alpha2M6)\,] \quad (8)$$

which evaluates to $mM6 \approx 75.6\%$. It is worth being direct about what this number is: it is not derived independently of the result it is meant to explain. *mM6* is solved for specifically so that the model's prediction matches the one data point — Sitaraman et al.'s (2015) −53.8% — that it is being asked to reproduce, and it carries no information beyond what was used to fit it. In the most literal sense, this is an *ad hoc* parameter: a free knob turned, after the fact, until the model agrees with the observation, rather than a quantity predicted in advance. A large, but not implausible, degree of feed-forward inhibitory suppression at full sleep deprivation is what the shared-*k* hypothesis *requires* if it is to survive at this node; whether MVP2, or anything else, actually supplies that much additional inhibition during sleep deprivation is a separate empirical question, taken up in Sections 5.3.4 and 5.3.5 below, and is not established by the fitting procedure itself.

As an internal consistency check, the same shared *k* was also applied to MVP2/γ1pedc's own α2 and GRASP data (measured in this thesis but not used to fit *k* or *m*), using equations (1)–(5) with no inhibitory term (MVP2 is the source of inhibition in this model, not a target of it):

$$A_{MVP2}(1) = (1 + \Delta graspMVP2) \cdot (1 + k \cdot \Delta\alpha2MVP2) \quad (9)$$

With an unchanged GRASP signal at this compartment (Weiss and Donlea, 2021) and the α2 increase measured here (+16.4%), this predicts MVP2's own output increases by roughly 2.6-fold at full sleep deprivation — the same order of magnitude as the 2.3-fold increase directly observed at γ2α′1. This is not an independent validation of the specific 75.6% inhibition figure, but it is an encouraging sign that the same shared mechanism, applied without modification to a third, previously unused data point, lands in a physiologically plausible range rather than an implausible one.

Combining the above, the complete forward model used to simulate all three nodes across the deprivation axis $s \in [0, 1]$ is:

$$A_{M6}(s) = (1 + \Delta graspM6 \cdot s) \cdot (1 + k \cdot \Delta\alpha2M6 \cdot s) \cdot (1 - mM6 \cdot s) \quad (10)$$

$$A_{\gamma2}(s) = (1 + \Delta grasp\gamma2 \cdot s) \cdot (1 + k \cdot \Delta\alpha2\gamma2 \cdot s) \quad (11)$$

$$A_{MVP2}(s) = (1 + \Delta graspMVP2 \cdot s) \cdot (1 + k \cdot \Delta\alpha2MVP2 \cdot s) \quad (12)$$

with the single shared parameter *k* = *+9.63* and the node-specific empirical inputs from Table 5.1, plus the fitted inhibition strength *mM6* = *0.756*.

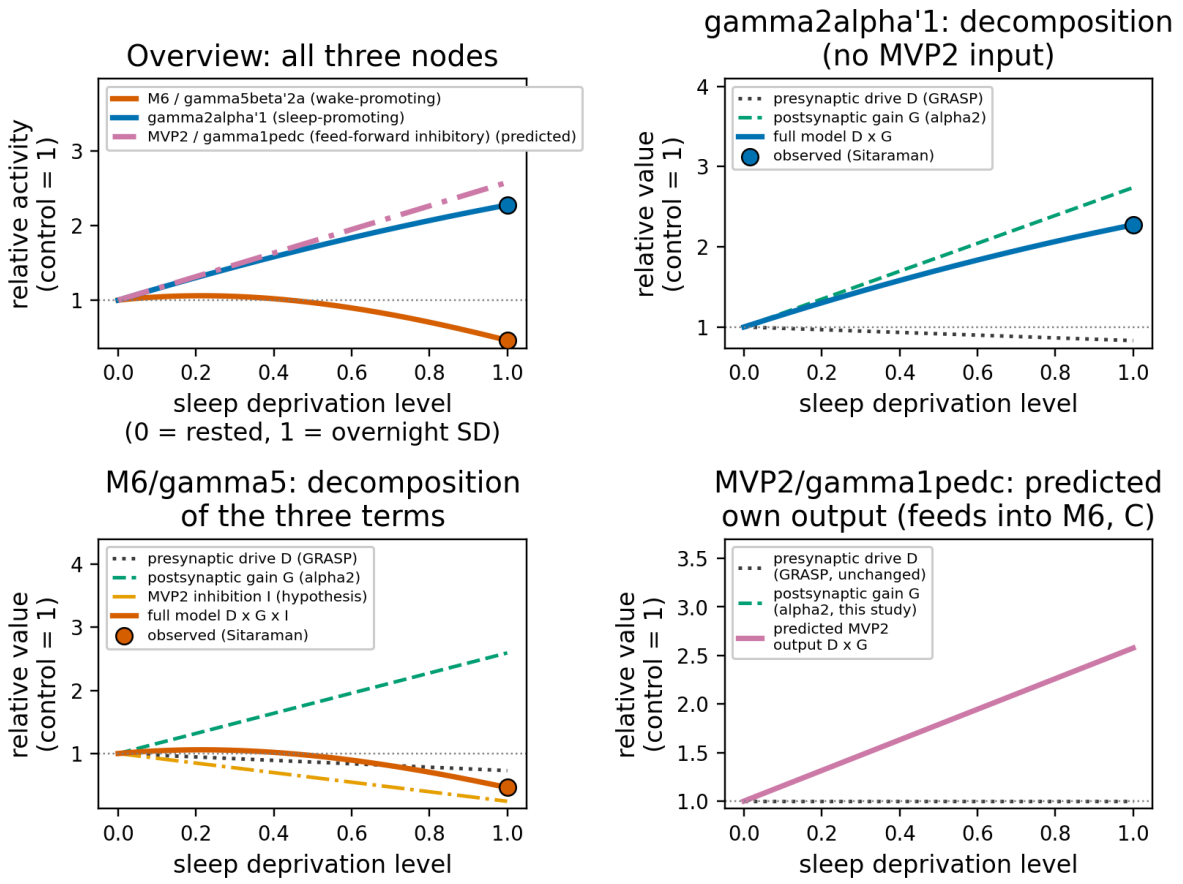


Figure 5.4 The full model (equations 10–12) across the sleep-deprivation axis, with the fitted MVP2 inhibition term included. Top left: all three nodes together — γ2α'1 (sleep-promoting) and the MVP2/γ1pedc prediction both increase; M6/γ5β'2a (wake-promoting) decreases once inhibition is included, matching Sitaraman et al. (2015) at s = 1 (filled circles). Top right and bottom left: term-by-term decomposition for γ2α'1 and M6/γ5β'2a respectively, showing the presynaptic (D), postsynaptic (G), and, for M6/γ5, inhibitory (I) components separately. Bottom right: the model's predicted output for MVP2/γ1pedc itself, used as the internal consistency check described in the text.

5.3.4 A speculative, same-dataset rationale for the MVP2 hypothesis

Given that *mM6* is fitted rather than measured, it is worth asking whether anything in the present dataset offers even indirect support for the idea that MVP2's inhibitory output specifically increases during sleep deprivation, rather than the inhibition term being an entirely unmotivated free parameter. One observation is directly relevant: γ1, the compartment corresponding to MVP2's own dendritic field, itself shows a significant α2-EGFP increase under sleep deprivation in this thesis's own data (+16.4%, Dunnett p = 0.042; Section 4.1). Applying the same interpretive logic used throughout this thesis for γ2α′1 and M6/γ5β′2a — that an α2 increase reflects increased postsynaptic gain at that neuron's own KC input — this same reasoning,

applied to MVP2 itself, would mean that MVP2 receives a larger postsynaptic response to a given amount of presynaptic KC drive under sleep deprivation.

MVP2 (MBON-γ1pedc) is a GABAergic interneuron with an established feed-forward inhibitory projection onto the M4/M6 group of MBONs, including M6/γ5β′2a (Perisse et al., 2016). If MVP2's own inhibitory output scales, even loosely, with the postsynaptic drive it receives from its KC inputs, a larger dendritic response under sleep deprivation could plausibly translate into a stronger inhibitory signal delivered downstream, onto exactly the node the model requires additional inhibition at. This is a genuinely distant and qualitative argument, not a quantitative one: it does not predict, or in any way constrain, the specific 75.6% inhibition figure the model requires, and the step from "more postsynaptic gain at MVP2's own dendrites" to "more inhibitory output at MVP2's axon terminals" is not demonstrated anywhere in this thesis, nor, to the author's knowledge, in the published literature. What it does provide is a same-dataset, same-mechanism reason to think that an increase in MVP2 inhibitory tone during sleep deprivation is not simply a convenient assumption introduced to rescue the model, but is at least directionally consistent with something this thesis independently measured at MVP2's own synapses.

5.3.5 An open experimental question

The MVP2 inhibition hypothesis, however it is motivated, remains untested. A literature search specifically for evidence that MVP2/γ1pedc's inhibitory output or activity changes during sleep deprivation did not identify any published study addressing this question directly. The existing literature on MVP2 establishes its feed-forward inhibitory projection onto the M4/M6 MBON group and its role in aversive and appetitive memory processing, including an increase in its own odor-evoked activity in hungry flies (Perisse et al., 2016) — but neither Sitaraman et al. (2015) nor Weiss and Donlea (2021), nor, as far as the author is aware, any other published study, measured MVP2's activity, output, or synaptic strength under sleep deprivation specifically.

This absence is itself informative: it means the MVP2 hypothesis proposed here is not a restatement of an existing finding but a genuinely new prediction generated by the modeling exercise, and one that is, at least in principle, directly testable. Testing it would require recording MVP2's own electrical activity — for instance with ArcLight,

the same reporter Sitaraman et al. (2015) used at γ2α′1 and M6/γ5β′2a — or measuring its GRASP-labeled synaptic contact onto M6/γ5β′2a, under the same sleep deprivation protocol used throughout this thesis, and asking whether either quantity increases in the way the model requires. This is a natural next step raised directly by the modeling work reported here, and is returned to in the Future Directions section of this chapter.

5.3.6 Assumptions and limitations of the model

This model is deliberately minimal, and its limitations are more consequential than its fit. Its inputs are approximate: the GRASP and ArcLight values were read from published figures rather than obtained as raw data (Section 5.3.1), and the three datasets combined here were collected in different studies, different animals, and different laboratories, which the model treats as compatible fractional-change estimates without independent justification. Its structure is static rather than dynamic: *s* interpolates linearly between two measured endpoints (rested control and full overnight deprivation) and does not capture the time course of onset, accumulation, or recovery of sleep pressure. Its central mechanistic claim — a single coupling constant *k* shared across structurally distinct MBON compartments — is a simplifying hypothesis motivated by parsimony, not an independently established biophysical fact, and everything downstream of it, including the specific *mM6* value, inherits this assumption. The MVP2 inhibition strength in particular is a fitted quantity required for internal consistency, not a measured property of MVP2 activity under sleep deprivation, which has not been directly recorded by any study to date. The same-dataset rationale offered in Section 5.3.4 — that MVP2's own α2 increase might plausibly translate into stronger inhibitory output — does not change this: it is a qualitative plausibility argument built on an assumption (that MVP2's output scales with its own postsynaptic drive) that is itself untested, and it should not be mistaken for evidence that the fitted 75.6% figure is correct.

None of this is incidental to how the model should be used. It is not offered as a validated, quantitative account of this circuit, and it is not intended to be — it is a small, transparent tool for asking a specific question (is a shared postsynaptic mechanism quantitatively compatible with the presynaptic and activity data at hand?), and for making explicit, in a single fitted number, exactly what additional

assumption is required if the answer is to be yes. That the answer, worked out this way, points specifically to MVP2-mediated inhibition — rather than remaining a vague, unstructured appeal to "compensation" — is the model's main contribution at this stage: it converts a qualitative plausibility argument into a specific, quantitative, and in principle falsifiable hypothesis, developed independently of the project's original experimental scope and still being actively refined.

Taken together, and despite the limitations just described, the modeling work in this section converges on a single, specific conclusion: reconciling the presynaptic, postsynaptic, and electrophysiological evidence available at MBON-γ5β′2a/M6 requires an additional source of inhibition, and MVP2 is the most anatomically plausible candidate for supplying it. Whatever weight one gives to the qualitative, same-dataset rationale offered in Section 5.3.4, the central hypothesis this chapter arrives at is that MVP2's inhibitory tone onto its downstream targets, including M6/γ5β′2a, increases during sleep deprivation. Framed this way, the hypothesis is not an endpoint but a starting point: it turns a modeling exercise into a concrete, testable prediction, and opens a specific line of experimental work aimed at directly recording or manipulating MVP2 activity and output under sleep deprivation. More broadly, pursuing that question would help map, in more functional and mechanistic detail than this work alone can provide, how postsynaptic plasticity is organized within the wider circuitry linking sleep homeostasis, sleep control, and learning and memory in the mushroom body — the same circuitry this thesis set out, in Chapter 1, to ask a first question about.

6. Conclusions

This thesis set out, in Chapter 2, to test whether sleep deprivation alters postsynaptic α2 nAChR subunit expression across the mushroom body output layer, whether any such effect is specific to sleep pressure or is instead shaped by feeding state, and whether the resulting pattern can be reconciled, quantitatively rather than only qualitatively, with the presynaptic and electrophysiological evidence already published for this circuit. The results reported in Chapters 4 and 5 answer all three questions. Sleep deprivation significantly increases α2-EGFP fluorescence at four of the ten compartments surveyed — γ5, γ2, γ1, and β1 — in a pattern that is compartment-specific rather than a generic consequence of the deprivation protocol. This effect is gated by feeding state: it is present in fed, sleep-deprived flies and absent when sleep deprivation is combined with food deprivation, an interaction that appears to reflect a genuine gating mechanism rather than a simple loss of statistical power. And at MBON-γ5β′2a/M6, where the direction of the α2 increase is, at face value, difficult to reconcile with this node's reported decrease in electrical activity, a dedicated computational model shows that this reconciliation is only possible if an additional source of inhibition — plausibly supplied by MVP2 neurons — is added to the local, α2-driven account, converting what began as a qualitative puzzle into a specific, testable hypothesis. What follows takes stock of what this approach can and cannot establish, and where it points next.

6.1 Limitations

The first limitation concerns the reporter itself. Postsynaptic α2 expression was measured using an endogenously EGFP-tagged α2 nAChR allele (Section 3.1), in which the fluorescent tag is inserted at the native locus and is therefore expressed constitutively, by every α2-expressing neuron in the brain, rather than being restricted by design to the specific KC-to-MBON synapses of interest. Because of this, the fluorescence measured within a given region of interest (ROI) cannot be attributed with certainty to postsynaptic α2 receptors at that compartment's KC input alone: it will also include some contribution from α2 expressed in cell bodies, dendrites, or passing neurites of other neurons that happen to occupy the same imaged volume. This is a genuine limitation of the underlying genetic strategy, and it means the fluorescence signal is not a pure, single-source readout of postsynaptic

receptor density at the synapse of interest. The working assumption that makes the approach useful despite this is not that the signal is pure, but that it is directionally informative: a change in mean ROI fluorescence between conditions should still track, on average, a real change in α2 expression at that compartment, even if the absolute signal at any single time point is a mixture of several sources. Two features of the dataset itself offer indirect support for this assumption. First, the effect is compartment-specific rather than global — six of the ten compartments sampled showed no significant change at all, which would not be expected if the signal were dominated by a nonspecific, brain-wide confound rather than by something happening locally at each compartment. Second, within a single neuron, MBON-γ5β′2a, only one of its two dendritic zones (γ5) showed a significant change while the other (β′2) did not (Section 4.1) — a degree of spatial specificity that is difficult to reconcile with substantial cross-contamination from neighboring or passing processes. Neither observation eliminates the limitation, but both make it less likely that the reported effects are simply an artifact of the reporter's constitutive expression.

A second limitation concerns how the ROIs themselves were defined. Quantification was performed in Fiji/ImageJ, with each of the ten mushroom body compartments outlined by hand using the freehand ROI tool, re-drawn from anatomical landmarks separately for every brain (Section 3.3). This was done by me, throughout the entire dataset, without an automated or machine-learning-based segmentation step to standardize ROI boundaries across brains and conditions. Manual ROI delineation of this kind is inevitably subject to a degree of human variability — in exactly where a boundary is drawn, and potentially in how consistently that boundary is drawn across different dissection days or experimental rounds — that a fully automated pipeline would reduce, though not eliminate. This is a limitation of the analysis pipeline as implemented here, rather than of the underlying biological measurement, and it is one that future iterations of this kind of quantification could directly address (Section 6.2).

A third limitation is sample size. Final group sizes, after collapsing technical replicates within each fly (Section 3.4), were CNTRL = 14, FD = 14, SD = 19, and FDSD = 20 flies. These are workable sample sizes for the comparisons reported

here, but they are not large by the standards of the field, and a larger sample — particularly for the two smaller groups, CNTRL and FD — would have provided more power to detect smaller effects and would have narrowed the confidence intervals around the estimates this thesis relies on, including the fractional changes that feed directly into the quantitative model of Section 5.3. This limitation is best understood as a consequence of the thesis's timeline rather than of the experimental design itself: learning the dissection, imaging, and quantification pipeline from scratch and then executing it across four conditions and multiple experimental rounds, within the timeframe available for this project, left less room than would have been ideal for scaling up the final sample size.

A fourth limitation concerns the sex of the animals sampled. Dissections were performed exclusively on female flies (Section 3.3), a practical and common choice in this field, but one that means this thesis cannot itself speak to whether the same effects hold in males. Sex-specific differences have been documented in some Drosophila circuits, particularly those tied to courtship and reproductive behavior, so this is a real question worth testing rather than a formality. However, the mechanism under study here — postsynaptic receptor-level plasticity at a cholinergic synapse, responding to a basic physiological pressure like sleep need — is not itself part of that sex-specific circuitry, and homeostatic synaptic scaling of this general kind is typically treated as a conserved, core property of neurons rather than a sexually dimorphic one. There is therefore good reason to expect the postsynaptic mechanism described in this thesis to generalize to males, even though confirming this directly remains a straightforward and worthwhile extension of the present work.

A fifth limitation is that every measurement in this thesis is a single-timepoint, endpoint snapshot — α2 expression compared between control and one fixed duration of sleep and/or food deprivation — rather than a time course. This design can establish that a difference exists between rested and sleep-deprived states, but it cannot say how quickly the α2 change develops over the course of sleep deprivation, whether it would grow further with a longer deprivation protocol, or how quickly it resolves once flies are allowed to recover sleep. The quantitative model in Section 5.3 inherits this same limitation directly: its sleep-deprivation axis, s, is a

linear interpolation between two measured endpoints, not a fitted or validated time course, and nothing in the present dataset constrains what happens between them.

A sixth limitation, restated here rather than left implicit, concerns the quantitative model developed in Section 5.3. Its inputs are approximate: the GRASP and ArcLight values it relies on were read directly off published bar-chart figures rather than obtained as raw data, because the original numeric values were not available from either source (Section 5.3.1). This is not a trivial rounding concern — it means every downstream quantity in the model, from the fitted coupling constant *k* to the fitted MVP2 inhibition strength *m*, inherits whatever imprecision comes from reading values off a printed figure rather than working from the authors' original numbers.

An eighth limitation is that the model combines measurements that were never collected together. The GRASP, α2, and ArcLight values feeding into it come from three different studies, conducted in different laboratories, in different years, using different transgenic reporters and different animals, and the model necessarily treats them as compatible fractional-change estimates for the same underlying nodes (Section 5.3.1). This is a working assumption adopted for lack of a better alternative, not an established fact, and it means the model should be read as a test of internal quantitative consistency given the best available approximations, rather than as an analysis of a single, jointly collected dataset.

A ninth limitation concerns the model's central addition at MBON-γ5β′2a/M6: an inhibitory term attributed to MVP2, with strength $m \approx 75.6\%$ (Section 5.3.3). This value is fitted specifically to reproduce the one observation it is meant to explain — Sitaraman et al. 's (2015) reported activity decrease at this node — rather than derived or measured independently of it. It should not be read as an implicit validation of the specific 75.6% figure, nor of MVP2 as the source of the missing inhibition as opposed to some other, unconsidered mechanism; it is, transparently, an *ad hoc* parameter, adopted because the model does not work without some term of this kind, not because independent evidence pointed to this exact value beforehand.

None of these three limitations is a minor caveat, and taken together they mean the model cannot be treated as a validated, quantitative account of this circuit. What it

does establish, despite them, is a more modest but still useful negative result: given the best available estimates of GRASP and activity change at MBON-γ5β′2a/M6, a purely local, presynaptic-plus-postsynaptic account is not merely insufficient but quantitatively incompatible with the observed decrease in activity, and some additional source of suppression is required to close that gap. A qualitative argument alone could never have shown this; only putting numbers to the claim could. That is the sense in which the modeling exercise, limitations included, represents a genuine advance over the purely descriptive alternative, even though it stops well short of demonstrating that MVP2 is, in fact, the source of that suppression.

A tenth and final limitation is one of scope rather than of execution. The project was originally envisaged as potentially extending to in vivo calcium imaging, using the same sleep deprivation, food deprivation, and combined food-and-sleep deprivation paradigm developed for the α2-EGFP experiments, to record MBON activity directly and ask whether it shifted in the same direction, and by a comparable magnitude, as the electrophysiological changes reported by Sitaraman et al. (2015) and the α2 changes reported in this thesis. This would have offered a direct, within-thesis test of the same reconciliation question that Section 5.3's model addresses only indirectly, using data collected under a single, consistent protocol rather than combined across studies. It was not possible to carry out this additional set of experiments within the time available for learning and executing the dissection, imaging, and quantification pipeline described in Chapter 2, and it remains, for now, an unrealized rather than an abandoned aim.

6.2 Future directions

The most direct extension of this work is the in vivo calcium imaging experiment described above: recording MBON activity under the same CNTRL/SD/FD/FDSD design used throughout this thesis would test, within a single consistent dataset, whether the direction and approximate magnitude of the activity changes match those inferred indirectly here from α2 expression and from Sitaraman et al.'s (2015) ArcLight recordings, and would do so without the cross-study compatibility assumptions that the model in Section 5.3 is forced to make.

Closely related to the calcium imaging experiment above is a second, complementary design already considered during this project but not carried out: a recovery time-course experiment, in which sleep-deprived flies are, after the standard deprivation protocol, allowed to sleep again, and α2-EGFP expression is then measured at successive time points afterward rather than only at the single post-deprivation endpoint used throughout this thesis. This would directly establish how long the α2 increase reported here persists once flies are permitted to recover sleep, and whether it decays back toward baseline on a timescale consistent with the resolution of sleep pressure itself. Recovery sleep is the classical test of whether a change is genuinely homeostatic rather than an incidental side effect of the deprivation protocol: a postsynaptic response that reliably reverses once sleep debt is repaid would be strong independent support for the homeostatic framing this thesis adopts throughout (Section 5.1), whereas a change that persisted regardless of recovery sleep would call that framing into question and point toward a different interpretation altogether.

A third, complementary priority is testing the MVP2 inhibitory-tone hypothesis directly (Section 5.3.5), since it is currently the central untested claim this thesis puts forward. This would mean recording MVP2's own electrical activity — for instance with ArcLight, the same reporter Sitaraman et al. (2015) used at the two other nodes modeled here — or measuring its GRASP-labeled synaptic contact onto M6/γ5β′2a, under the same sleep deprivation protocol, to ask directly whether either quantity increases in the way the fitted model requires.

A fourth priority is testing the GRASP-α2 feedback hypothesis introduced in Section 5.1 directly, rather than inferring it from the co-occurrence of two independently collected datasets. This would require tracking both GRASP contact number and α2 density in the same animals — ideally across the time course of sleep deprivation and subsequent recovery sleep — to establish whether the two changes co-occur within individual flies, or manipulating one side of the proposed loop directly (for instance, genetically altering KC-to-MBON contact number at a single compartment) and asking whether α2 density at that same compartment responds accordingly.

A fifth priority follows directly from the hunger-gating result of Section 5.2, and is really three linked experiments rather than one. The first is to quantify total sleep loss

and its time course directly in FDSD flies, rather than assuming, as this thesis necessarily did, that mechanically sleep-deprived FDSD flies lose sleep to the same degree as SD flies simply because the same deprivation apparatus was applied to both. This matters because Keene et al. (2010) showed that starvation-induced wakefulness in *Drosophila* does not behave like ordinary sleep deprivation — it produces no compensatory rebound and depends on a distinct, clock-gene-dependent circuit — so it remains genuinely open whether an FDSD fly accumulates the same homeostatic sleep pressure as an SD fly, or simply stays awake for a different reason that happens to look similar from the outside. Confirming or ruling out a behavioral difference of this kind is a precondition for interpreting the FDSD null result as gating rather than as a difference in how effectively the two protocols deprive flies of sleep in the first place.

The second experiment in this group is to manipulate Neuropeptide F signaling specifically, while holding the sleep and food deprivation protocols themselves fixed, and ask whether doing so changes the FDSD result. NPF is independently required for starvation-induced wakefulness and feeding in *Drosophila* (Chung et al., 2017), which makes it the most concrete candidate so far for a molecular link between the hunger and sleep-homeostat pathways discussed in Section 5.2 — rather than two pathways that merely compete for the fly's behavioral output without any point of contact between them. If knocking down NPF signaling in FDSD flies restored the α2 increase that fed, sleep-deprived flies show, that would be direct evidence that this specific hunger signal, and not hunger in general, is what gates the postsynaptic response; if it did not, that would argue for a different, NPF-independent route between the two systems.

The third experiment is to extend the anatomical survey beyond the ten mushroom body compartments sampled in this thesis, to include circuits outside the mushroom body itself — in particular the dorsal clock-neuron population that Keene et al. (2010) implicate in starvation-induced wakefulness. Section 5.2 could not distinguish between two accounts of the FDSD null result: a Chouhan-style circuit switch, in which the physiological consequences of lost sleep are rerouted away from the mushroom body entirely under hunger, and a Keene-style upstream uncoupling, in which those consequences are simply not generated in the first place because

hunger-driven wakefulness does not register as classical homeostatic sleep pressure. Looking for a postsynaptic signature of lost sleep in the clock-neuron circuit itself, under the same FDSD protocol, is a direct way to ask whether the two accounts can be told apart: finding one there would favor rerouting, and finding none anywhere would favor upstream uncoupling.

A sixth priority is simply a larger sample size than the one this thesis was able to collect. This would help in two distinct ways. It would give more power to detect real but modest effects in the raw compartment-by-compartment comparisons themselves, particularly for the two smaller groups (CNTRL and FD, n = 14 each); and, because the fractional changes reported in Section 4.1 feed directly into the quantitative model of Section 5.3 as fixed inputs, a larger sample would also narrow the uncertainty around the model's own outputs — including the fitted coupling constant *k* and the fitted MVP2 inhibition strength *m* — rather than only around the underlying experimental comparisons.

A seventh priority is to replace the manual ROI segmentation described in Section 6.1 with a procedure less dependent on a single person's judgment. This could take the form of a convolutional segmentation model trained on the ROIs already hand-drawn for this thesis, used to standardize compartment boundaries across brains going forward, or, at minimum, a blinded re-tracing protocol in which compartment boundaries are drawn without the experimenter knowing which experimental group a given brain belongs to. Either approach would directly address the human-variability concern raised in Section 6.1, without requiring the underlying imaging protocol to change.

An eighth priority is to repeat this design in male flies. Every result in this thesis was obtained in females only (Section 6.1), and sex differences in *Drosophila* sleep and courtship circuitry are well documented; whether the same compartment-specific α2 increase, and the same hunger-dependent gating of it, is also present in males is a straightforward and, at present, entirely open empirical question.

A ninth priority, complementary to the recovery time-course experiment already described above, is to sample α2 expression at several points *during* sleep deprivation itself, rather than only at the single endpoint used throughout this thesis.

This would establish how quickly the α2 increase reported here actually develops over the course of a deprivation protocol, and whether a longer deprivation period would push it further still — the onset side of the same time-resolved picture that the recovery experiment addresses on the offset side.

A tenth and final priority is to test the postsynaptic mechanism causally rather than correlationally, by knocking down or overexpressing α2 at a single compartment — γ5 would be the natural first target, given the specific puzzle it raises in this thesis — and asking whether this manipulation is, on its own, sufficient to shift that compartment's electrophysiological response to sleep deprivation. This is the single experiment that would most directly convert the central claim of this thesis from a correlation, however well contextualized, into a demonstrated causal mechanism.

Taken together, these are not small additions to a finished picture but the specific next steps this thesis's own results point to. Some follow directly from a hypothesis this thesis generated but could not itself test — the in vivo calcium imaging study and the recovery time-course experiment that the original project envisaged but could not complete, and the direct test of MVP2's inhibitory tone that the quantitative model now makes precise and falsifiable. Others follow from a result this thesis could describe but not fully explain — the mechanistic dissection of how feeding state gates the sleep-deprivation response, and the direct test of the GRASP-α2 feedback hypothesis itself. And others follow from the limitations catalogued in Section 6.1 — a larger and more balanced sample, a less experimenter-dependent quantification pipeline, a time-resolved design, and a causal rather than correlational test of the postsynaptic mechanism. Each, in its own way, would help build a more complete, and more directly causal, account of how postsynaptic plasticity at KC-to-MBON synapses contributes to the broader circuitry linking sleep homeostasis, sleep control, and learning and memory in the mushroom body.

What this thesis set out to do was ask a single, narrow question — whether a postsynaptic nicotinic receptor subunit changes in response to internal state pressure at identified mushroom body output synapses — and it answers that question with real, if imperfect, evidence: a compartment-specific effect, a previously undescribed interaction with feeding state, and a quantitative reason to think that a still-unconfirmed inhibitory input completes the picture at the one node where the

simplest account fails. None of these results closes its own question so much as sharpens it into one that can now be asked more precisely, and with better tools, than it could be at the outset of this project. If the broader ambition behind this work — understanding how single synapses within a defined circuit adjust their own strength in response to an animal's internal state — is worth pursuing further, it is because the mushroom body keeps offering exactly this kind of opening: a circuit small and well-mapped enough that a specific, falsifiable hypothesis about one interneuron's inhibitory output is now a realistic experiment, not a distant one.

References

Abraham, W.C. and Bear, M.F. (1996). Metaplasticity: the plasticity of synaptic plasticity. *Trends in Neurosciences*, 19(4), 126–130. *[1.4]*

Aso, Y., Hattori, D., Yu, Y., Johnston, R.M., Iyer, N.A., et al. (2014). The neuronal architecture of the mushroom body provides a logic for associative learning. *eLife*, 3, e04577. *[2.3 (figure)]*

Aso, Y., Sitaraman, D., Ichinose, T., Kaun, K.R., Vogt, K., et al. (2014). Mushroom body output neurons encode valence and guide memory-based action selection in *Drosophila*. *eLife*, 3, e04580. *[1.2, 1.3, 1.4]*

Bargmann, C.I. and Marder, E. (2013). From the connectome to brain function. *Nature Methods*, 10(6), 483–490. *[1.1]*

Barnstedt, O., Owald, D., Felsenberg, J., Brain, R., Moszynski, J.P., Talbot, C.B., Perrat, P.N. and Waddell, S. (2016). Memory-relevant mushroom body output synapses are cholinergic. *Neuron*, 89(6), 1237–1247. *[1.2, 1.3]*

Bellen, H.J., Tong, C. and Tsuda, H. (2010). 100 years of *Drosophila* research and its impact on vertebrate neuroscience: a history lesson for the future. *Nature Reviews Neuroscience*, 11, 514–522. *[1.2]*

Béïque, J.C., Na, Y., Kuhl, D., Worley, P.F. and Huganir, R.L. (2011). Arc-dependent synapse-specific homeostatic plasticity. *Proceedings of the National Academy of Sciences*, 108(2), 816–821. *[5.1]*

Bliss, T.V.P. and Lømo, T. (1973). Long-lasting potentiation of synaptic transmission in the dentate area of the anaesthetized rabbit following stimulation of the perforant path. *Journal of Physiology*, 232(2), 331–356. *[1.1]*

Brand, A.H. and Perrimon, N. (1993). Targeted gene expression as a means of altering cell fates and generating dominant phenotypes. *Development*, 118(2), 401–415. *[1.2]*

Changeux, J.P. and Danchin, A. (1976). Selective stabilisation of developing synapses as a mechanism for the specification of neuronal networks. *Nature*, 264(5588), 705–712. *[1.1]*

Chouhan, N.S., Griffith, L.C., Haynes, P. and Sehgal, A. (2020). Availability of food determines the need for sleep in memory consolidation. *Nature*, 589, 582–585. *[1.4, 2 (Aim 2), 5.2]*

Chung, B.Y., Ro, J., Hutter, S.A., Miller, K.M., Guduguntla, L.S., Kondo, S. and Pletcher, S.D. (2017). *Drosophila* neuropeptide F signaling independently regulates feeding and sleep-wake behavior. *Cell Reports*, 19(12), 2441–2450. *[5.2, 6.2]*

Cohn, R., Morantte, I. and Ruta, V. (2015). Coordinated and compartmentalized neuromodulation shapes sensory processing in *Drosophila*. *Cell*, 163(7), 1742–1755. *[1.3]*

Davis, G.W. (2006). Homeostatic control of neural activity: from phenomenology to molecular design. *Annual Review of Neuroscience*, 29, 307–323. *[5.1]*

Dupuis, J., Louis, T., Gauthier, M. and Raymond, V. (2012). Insights from honeybee (*Apis mellifera*) and fly (*Drosophila melanogaster*) nicotinic acetylcholine receptors: from genes to behavioral functions. *Neuroscience & Biobehavioral Reviews*, 36(6), 1553–1564. *[1.3]*

Glanzman, D.L. (2010). Common mechanisms of synaptic plasticity in vertebrates and invertebrates. *Current Biology*, 20(1), R31–R36. *[1.3]*

Gundelfinger, E.D. and Hess, N. (1992). Nicotinic acetylcholine receptors of the central nervous system of *Drosophila*. *Biochimica et Biophysica Acta*, 1137(3), 299–308. *[1.3]*

Hebb, D.O. (1949). *The Organization of Behavior: A Neuropsychological Theory*. New York: John Wiley & Sons. *[1.1]*

Hensch, T.K. (2005). Critical period plasticity in local cortical circuits. *Nature Reviews Neuroscience*, 6(11), 877–888. *[1.1]*

Hige, T., Aso, Y., Modi, M.N., Rubin, G.M. and Turner, G.C. (2015). Heterosynaptic plasticity underlies aversive olfactory learning in *Drosophila*. *Neuron*, 88(5), 985–998. *[1.3]*

Ihara, M., Furutani, S., Shigetou, S., Shimada, S., Niki, K., et al. (2020). Cofactor-enabled functional expression of fruit fly, honeybee, and bumblebee nicotinic receptors reveals picomolar neonicotinoid actions. *Proceedings of the National Academy of Sciences*, 117(28), 16283–16291. *[1.3]*

Kandel, E.R. (2001). The molecular biology of memory storage: a dialogue between genes and synapses. *Science*, 294(5544), 1030–1038. *[1.1]*

Katz, L.C. and Shatz, C.J. (1996). Synaptic activity and the construction of cortical circuits. *Science*, 274(5290), 1133–1138. *[1.1]*

Keene, A.C., Duboué, E.R., McDonald, D.M., Dus, M., Suh, G.S.B., Waddell, S. and Blau, J. (2010). Clock and *cycle* limit starvation-induced sleep loss in *Drosophila*. *Current Biology*, 20(13), 1209–1215. *[5.2, 6.2]*

Korte, M. and Schmitz, D. (2016). Cellular and system biology of memory: timing, molecules, and beyond. *Physiological Reviews*, 96(2), 647–693. *[1.3]*

Landauer, T.K. (1986). How much do people remember? Some estimates of the quantity of learned information in long-term memory. *Cognitive Science*, 10(4), 477–493. *[1.1]*

Lansdell, S.J., Collins, T., Goodchild, J. and Millar, N.S. (2012). The *Drosophila* nicotinic acetylcholine receptor subunits Dα5 and Dα7 form functional homomeric and heteromeric ion channels. *BMC Neuroscience*, 13, 73. *[1.3]*

LeDoux, J. (2002). *Synaptic Self: How Our Brains Become Who We Are*. New York: Viking. *[1.1]*

Modi, M.N., Shuai, Y. and Turner, G.C. (2020). The Drosophila mushroom body: from architecture to algorithm in a learning circuit. *Annual Review of Neuroscience*, 43, 465–484. *[1.2]*

Nicoll, R.A. (2017). A brief history of long-term potentiation. *Neuron*, 93(2), 281–290. *[1.3]*

Owald, D. and Waddell, S. (2015). Olfactory learning skews mushroom body output pathways to steer behavioral choice in *Drosophila*. *Current Opinion in Neurobiology*, 35, 178–184. *[1.2, 1.3]*

Pfeiffer, B.D., Ngo, T.T.B., Hibbard, K.L., Murphy, C., Jenett, A., Truman, J.W. and Rubin, G.M. (2010). Refinement of tools for targeted gene expression in *Drosophila*. *Genetics*, 186(2), 735–755. *[1.2]*

Perisse, E., Owald, D., Barnstedt, O., Talbot, C.B., Huetteroth, W. and Waddell, S. (2016). Aversive learning and appetitive motivation toggle feed-forward inhibition in the *Drosophila* mushroom body. *Neuron*, 90(5), 1086–1099. *[5.3]*

Pribbenow, C., Chen, Y.C., Heim, M.M., Laber, D., Reubold, S., et al. (2022). Postsynaptic plasticity of cholinergic synapses underlies the induction and expression of appetitive and familiarity memories in *Drosophila*. *eLife*, 11, e80445. *[1.2, 1.3]*

Pribbenow, C. (2025). *Postsynaptic Plasticity of Cholinergic Synapses Underlying Learning in Drosophila* (Doctoral dissertation). Charité – Universitätsmedizin Berlin. *[1.3]*

Reiter, L.T., Potocki, L., Chien, S., Gribskov, M. and Bier, E. (2001). A systematic analysis of human disease-associated gene sequences in *Drosophila melanogaster*. *Genome Research*, 11(6), 1114–1125. *[1.2]*

Rosenthal, J.S. and Yuan, Q. (2021). Constructing and tuning excitatory cholinergic synapses: the multifaceted functions of nicotinic acetylcholine receptors in *Drosophila* neural development and physiology. *Frontiers in Cellular Neuroscience*, 15, 720560. *[1.3]*

Shomrat, T., Graindorge, N., Bellanger, C., Fiorito, G., Loewenstein, Y. and Hochner, B. (2011). Alternative sites of synaptic plasticity in two homologous 'fan-out fan-in' learning and memory networks. *Current Biology*, 21(21), 1773–1782. *[1.2, 1.3]*

Sitaraman, D., Aso, Y., Jin, X., Chen, N., Felix, M., Rubin, G.M. and Nitabach, M.N. (2015). Propagation of homeostatic sleep signals by segregated synaptic microcircuits of the *Drosophila* mushroom body. *Current Biology*, 25(22), 2915–2927. *[1.4, 1.5, 4.1, 5.1, 5.3, 6.1, 6.2]*

Tsao, C.H., Chen, C.C., Lin, C.H., Yang, H.Y. and Lin, S. (2018). *Drosophila* mushroom bodies integrate hunger and satiety signals to control innate food-seeking behavior. *eLife*, 7, e35264. *[1.4]*

Turrigiano, G.G., Leslie, K.R., Desai, N.S., Rutherford, L.C. and Nelson, S.B. (1998). Activity-dependent scaling of quantal amplitude in neocortical neurons. *Nature*, 391, 892–896. *[5.1]*

Weiss, J.T. and Donlea, J.M. (2021). Sleep deprivation results in diverse patterns of synaptic scaling across the *Drosophila* mushroom bodies. *Current Biology*, 31(15), 3248–3261. *[1.4, 1.5, 4.1, 5.1, 5.3]*

Zador, A.M. (2019). A critique of pure learning and what artificial neural networks can learn from animal brains. *Nature Communications*, 10, 3770. *[1.1]*